

Synthesis of Fluorinated Oligomers toward Physical Vapor Deposition Molecular Electronics Candidates

Francisco Maya,[†] Stéphanie H. Chanteau,[†] Long Cheng, Michael P. Stewart,[†] and James M. Tour*

Department of Chemistry and Center for Nanoscale Science and Technology, MS 222, Rice University, 6100 Main Street, Houston, Texas 77005

Received August 18, 2004. Revised Manuscript Received December 20, 2004

New electron-deficient fluorinated oligo(phenylene ethynylenes) (OPEs) with varied functional groups were synthesized as free thiols, nitriles, and pyridines, ready to be used for surface adhesion. Calculated dipole moments suggest better matching between energy levels of bulk interfaces and molecular frontier orbitals when compared to nonfluorinated OPEs. Differential scanning calorimetry confirmed a higher thermal stability than the nonfluorinated counterparts. Surface analysis by ellipsometry, contact angle goniometry, cyclic voltammetry, and surface infrared and X-ray photoelectron spectroscopy verified that the OPEs chemisorb on Au and Pt surfaces. On the basis of the physical properties of the fluorinated OPEs, they might be useful in future physical vapor deposition techniques, methods that are typically used in standard semiconductor fabrication processes.

1. Introduction

The development of electronic devices based on conjugated organic molecules has been one of the “bottom-up” approaches developed to address the present physical and economic limitations that arise as integrated circuits are miniaturized.¹ Through this approach, we have been pursuing molecular diversity by the rational design of linear conjugated oligomers that possess not only the conductive characteristics similar to those of previous molecular devices,² but also address specific challenges presented in the fabrication process of these electronic devices. To that end, we report here the synthesis of new oligo(phenylene ethynylene) (OPE) derivatives with a range of surface bonding moieties (alligator clips) and functional groups, including an electron-deficient polyfluoroarene. The objective with these new OPEs is to alter the thermal, chemical, and electronic properties of the molecules, to make them suitable for integration with solid-state devices. Such alterations may offer new benefits to electronic devices based on present fabrication approaches.

In general, the use of fluorocarbons as organic thin film precursors produces materials with increased thermal stability and chemical resistance. The intermolecular attractive forces become less dominant so that the molecular interactions at the chemical interface level become more pronounced compared to those of the nonfluorinated analogues.³ This is especially true for aromatic fluorine compounds.⁴ These characteristics could be critical for high-temperature pro-

cesses such as gas-phase physical vapor deposition (PVD).⁵ PVD at ultrahigh vacuum (UHV) has been pursued as an alternative to solution-phase formation of self-assembled monolayers (SAMs),⁶ and specifically as a method for the production of molecular electronic devices. For these electronic architectures that are assembled using PVD, the integrity and thermal stability of the organic layers are critical. This has been the case for pentafluorophenyl comonomers⁷ and vinyl monomers,⁸ among other oligomers,^{9,10} that have been used as candidates for dielectric and optical waveguide devices due their improved electronic properties.¹¹

With the goal of producing several new molecular electronics candidates that would be appropriate for PVD applications, we present the synthesis of nine oligomers shown in Figure 1. The central core of these oligomers has been functionalized with nitro or amine groups, which have been widely reported to act as redox centers for switching effects.²

The OPEs were functionalized with various alligator clips, including free thiols,^{12,13} nitriles,¹⁴ and pyridines^{15,16} for

* To whom correspondence should be addressed. E-mail: tour@rice.edu.

[†] Present address: Intel Corporation.

- (1) Tour, J. M. *Molecular Electronics: Commercial Insights, Chemistry, Devices, Architecture and Programming*; World Scientific: River Edge, NJ, 2003.
- (2) Chen, J.; Wang, J.; Reed, M. A.; Rawlett, A. M.; Price, D. W.; Tour, J. M. *Appl. Phys. Lett.* **2000**, *77*, 1224.
- (3) Olah, G. A. *Fluorine in Organic Chemistry, Interscience Monographs on Organic Chemistry*; John Wiley & Sons: New York, 1973.

- (4) Pavlath, A. E.; Leffler, A. J. *Aromatic Fluorine Compounds*; Reinhold Publishing Corporation: New York, 1962.
- (5) Chiang, L. Y.; Swirczewski, J. W.; Lai, F.; Goshorn, D. P. *Synth. Met.* **1991**, *41*, 1425.
- (6) Song, W. J.; Seoul, C.; Kang, G.-W.; Lee, C. *Synth. Met.* **2000**, *41*, 355.
- (7) Pitois, C.; Vukmirovic, S.; Hults, A.; Wiesmann, D.; Robertsson, M. *Macromolecules* **1999**, *32*, 2903.
- (8) Kim, J. P.; Lee, W. Y.; Kang, J. W.; Kwon, S. K.; Kim, J. J.; Lee, J. S. *Macromolecules* **2001**, *34*, 7817.
- (9) Elada, L. A.; Shacklette, L. W.; Norwood, R. A.; Yardley, J. T. *SPIE Crit. Rev.* **1997**, *CR68*, 207.
- (10) Kobayashi, J.; Matsuura, T.; Hida, Y.; Sasaki, S.; Maruno, T. J. *Lightwave Technol.* **1998**, *16*, 1024.
- (11) Wang, J.; Sustack, P.; Garner, S. *Proc. SPIE* **2002**, *129*, 4904.
- (12) Dhirani, A.; Lin, P.-H.; Guyot-Sionnest, P.; Zehner, R. W.; Sita, L. R. *J. Chem. Phys.* **1997**, *106*, 5249.
- (13) Cygan, M. T.; Dunbar, T. D.; Arnold, J. J.; Bumm, L. A.; Shedlock, N. F. *J. Am. Chem. Soc.* **1998**, *120*, 2721.

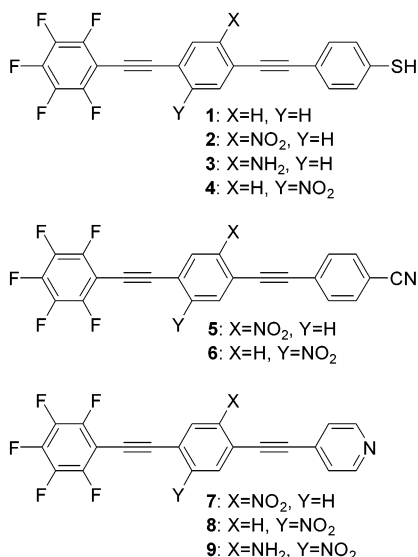


Figure 1. Fluorinated OPEs reported in this work.

making molecular scale junctions with several bulk contacts.¹⁷ Each new molecule contained an electron-deficient pentafluoro aromatic ring as the dipole moment director. Thermal analyses on these new oligomers were performed by differential scanning calorimetry (DSC) to gain insights into their thermal stability and their possible use in PVD processes. Theoretical values of their dipole moments and frontier orbital energies were calculated using density functional theory as explained in the Experimental Section.

Surface analysis of chemisorbed compounds on Au and Pt was performed by ellipsometry, contact angle goniometry, Fourier transform infrared (FTIR) analysis, and X-ray photoelectron spectroscopy (XPS).

2. Results

2.1. Theoretical Calculations. For conjugated linear molecules, it has been demonstrated that better control and improvement of electronic charge and hole injection is possible when utilizing fluorinated OPEs.¹⁸ Because of the lower intermolecular interaction, OPEs with fluorine substituents also demonstrated tighter molecular packing in SAMs¹⁹ and behaved as *n*-type organic semiconductors.²⁰ As reported by Campbell and co-workers,²¹ such electronic effects were possible by manipulating the Schottky energy barrier, which is the energy gap between the work function of the bulk interface and the molecular frontier orbitals. A high dipole moment driven by the electron-deficient fluori-

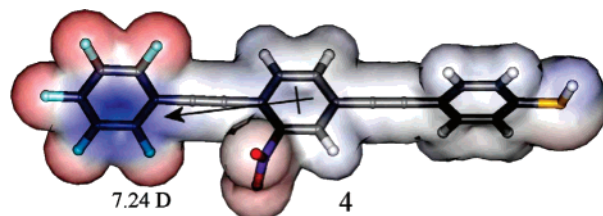


Figure 2. Electrostatic surface and dipole moment (7.24 D) for the OPE 4 with a fluorinated aromatic ring. Red and blue colors of the surface represent higher and lower electron densities respectively, indicating the high electronegativity that fluorines impart, and the electron-withdrawing nature of the nitro group. For a nonfluorinated OPE (not shown), the vector is smaller (3.1 D).

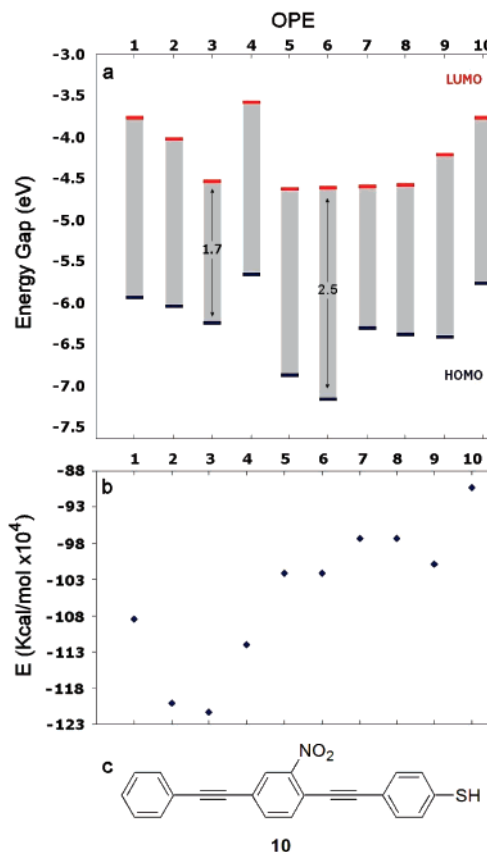
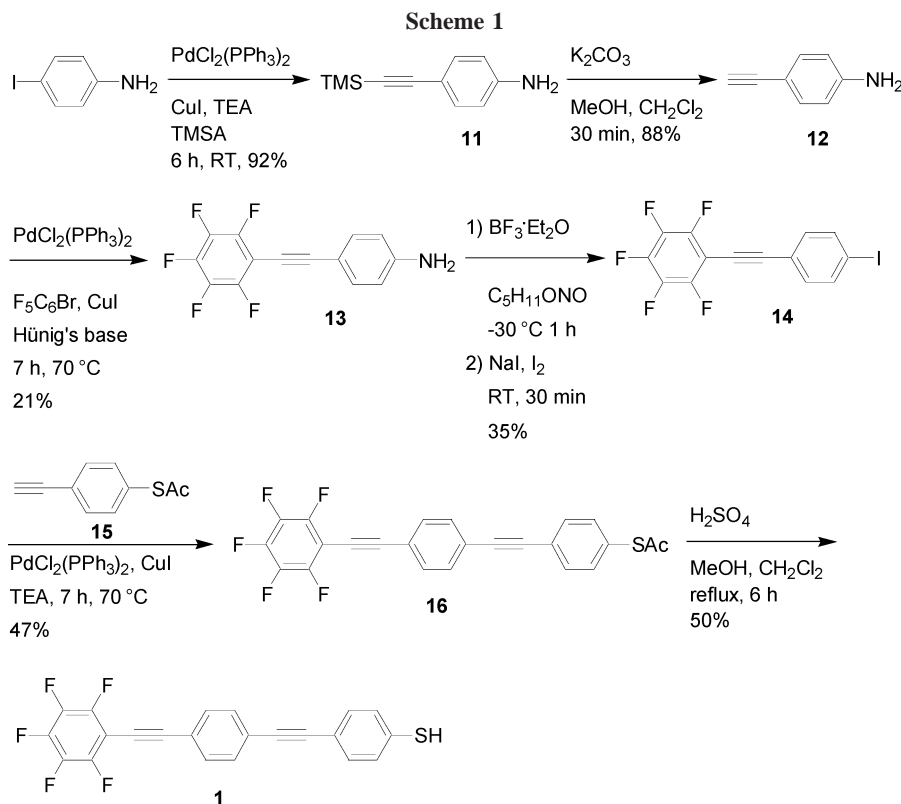


Figure 3. (a) Calculated energy gaps between the frontier orbitals and (b) total energy for every target presented in this work. (c) Chemical structure for OPE 10 included for comparison purposes.

nated ring in the opposite direction of the electrode contact was responsible for reducing the energy barrier, allowing for a more facile electronic flow.²¹ Using calculations, such dipole moments were also observed in our new targets as shown in Figure 2.

Figure 3 illustrates calculated energies of targets 1–9 and the energy gaps of their molecular orbitals. For comparison purposes, the same calculations were done for 4-(2-nitro-4-phenylethynylphenylethynyl)benzenethiol 10 (Figure 3c). Although the OPE 6 shows the largest energy gap, in general the LUMOs of all the molecules lie at a value equal to or lower than that of their nonfluorinated counterparts. Fluorinated compounds such as 4 may lower the HOMO energy and the corresponding Schottky energy barrier, increasing the electron transmission from a bulk contact through the frontier orbitals of a chemisorbed organic film.²²

- (14) Dirk, S. M.; Tour, J. M. *Tetrahedron* **2003**, 59, 287.
- (15) Chanteau, S. H.; Tour, J. M. *Tetrahedron Lett.* **2001**, 42, 3057.
- (16) Li, C.; Zhang, D.; Liu, X.; Han, S.; Tang, T.; Zhou, C.; Fan, W.; Koehne, J.; Han, J.; Meyyappan, M.; Rawlett, A. M.; Price, D. W.; Tour, J. M. *Appl. Phys. Lett.* **2003**, 82, 645.
- (17) Seminario, J. M.; De La Cruz, C. E.; Derosa, P. A. *J. Am. Chem. Soc.* **2001**, 123, 5616.
- (18) Campbell, I. H.; Kress, J. D.; Marting, R. L.; Smith, D. L.; Barashkov, N. N.; Ferraris, J. P. *Appl. Phys. Lett.* **1997**, 71, 3528.
- (19) Vondrak, T.; Cramer, C. J.; Zhu, X.-Y. *J. Phys. Chem. B* **1999**, 103, 8915.
- (20) Facchetti, A.; Yoon, M.-H.; Stern, C. L.; Katz, H. E.; Marks, T. J. *Angew. Chem., Int. Ed.* **2003**, 42, 3900.
- (21) Campbell, I. H.; Hagler, A. J.; Smith, D. L.; Ferraris, J. P. *Phys. Rev. Lett.* **1996**, 76, 1900.



The fluorinated mononitro OPE **2** shows a remarkable lower energy value (-120×10^4 kcal/mol) compared with its counterpart nonfluorinated OPE **10** (-90×10^4 kcal/mol, Figure 3b).

2.2. Synthesis. The synthesis of OPE **1** is presented in Scheme 1. Commercially available 4-iodoaniline was first coupled with trimethylsilylacetylene (TMSA) to afford **11**, which was then desilylated in alkaline methanol to furnish 4-ethynylaniline **12** as previously reported.²³

Coupling **12** with bromopentafluorobenzene via Sonogashira reaction²⁴ furnished aniline **13** which was converted to the iodide **14** in two steps: first, diazotization with isoamyl nitrite and boron trifluoride etherate, followed by iodination with sodium iodide and iodine. A second coupling with the free alkyne of the alligator clip **15**²⁵ gave the thioacetate **16**, followed by its acidic-deprotection with sulfuric acid, yielding the desired product **1** as a free thiol.

Although most of the synthetic steps gave only moderate yields, their relative simplicity and ease prompted us to use them for the synthesis of several different functionalized central cores and alligator clips. Scheme 2 illustrates the synthesis of the OPE **2** that includes a redox center; the nitro group having its origin as commercially available 2-nitroaniline. Iodination of this starting material with triethylbenzylammonium iodide dichloride provided **17**.²⁶

Aside from the direct iodination of the starting material, we used the same reagents and conditions from the previous OPE synthesis to afford the free alkyne nitroaniline **19**. Palladium-catalyzed coupling with F_5C_6Br afforded the fluorinated aniline **20**, which was then converted to the iodide **21** via diazotization, followed by iodination under typical conditions. A second coupling with 4-ethynylphenylthioacetate (**15**) gave the mononitro fluorinated oligomer **22**, which was finally deprotected under acidic conditions to yield the free thiol **2**.

Intermediate **21** made possible the synthesis of a variety of fluorinated oligomers with different functional groups and alligator clips. Scheme 3 shows the synthesis of an OPE that bears an amino group, an electron-donating moiety that will provide complementary electronic behavior compared to the OPE **2**.²⁵

The reduction of the nitro moiety on **21** was accomplished by treatment with tin(II) chloride, affording the iodoaniline **23**. Subsequent coupling with the free alkyne **15** and deprotection of the resulting thioacetate provided the desired aniline **3** as a free thiol.

An isomer of the fluorinated-mononitro OPE **2** was prepared as shown in Scheme 4. This time, the pentafluoro aromatic ring was prepared bearing a free alkyne by coupling first with TMSA to give **25**, followed by alkaline deprotection with KOH to obtain **26** as a light clear liquid.²⁷ The iodide intermediate **27**, which was produced by iodinating 3-nitroaniline with iodine monochloride, was ready for a Sonogashira coupling with **26**. This different approach unfortunately did not show an increased yield for the

(22) Fan, F. F.; Lai, R. Y.; Cornil, J.; Karzazi, Y.; Brédas, J.-L.; Cai, L.; Cheng, L.; Yao, Y.; Price, D. W., Jr.; Dirk, S. M.; Tour, J. M.; Bard, A. J. *J. Am. Chem. Soc.* **2004**, *126*, 2568.

(23) Dirk, S. M.; Price, D. W.; Chanteau, S. H.; Kosynkin, D. V.; Tour, J. M. *Tetrahedron* **2001**, *57*, 5109.

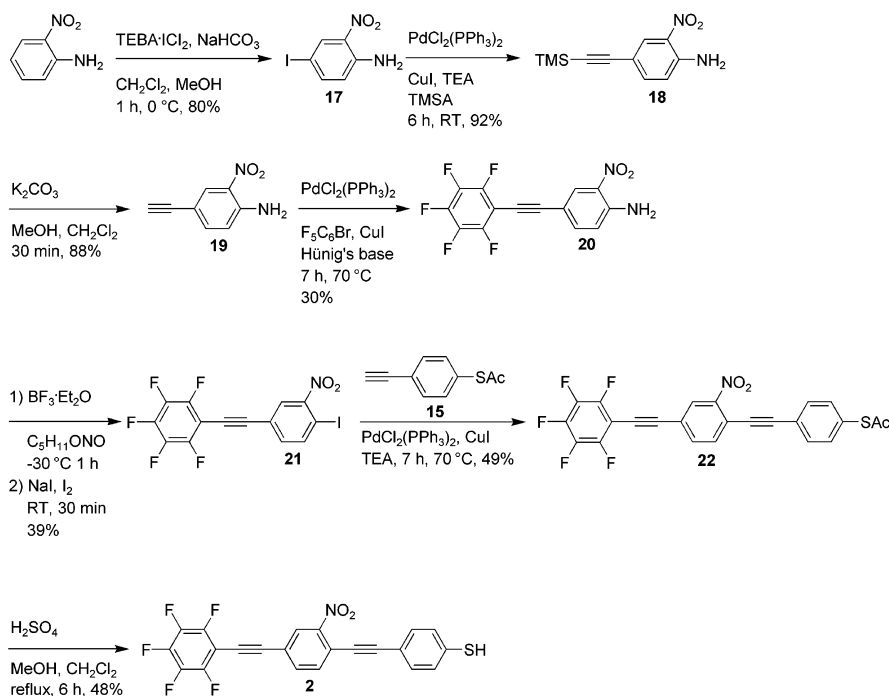
(24) Sonogashira, K.; Tohda, Y.; Hagihara, N. *Tetrahedron Lett.* **1975**, *50*, 4467.

(25) Tour, J. M.; Rawlett, A. M.; Kozaki, M.; Yao, Y.; Jagessar, R. C.; Dirk, S. M.; Price, D. W.; Reed, M. A.; Zhou, C.; Chen, J.; Wang, W.; Campbell, I. H. *Chem. Eur. J.* **2001**, *7*, 5118.

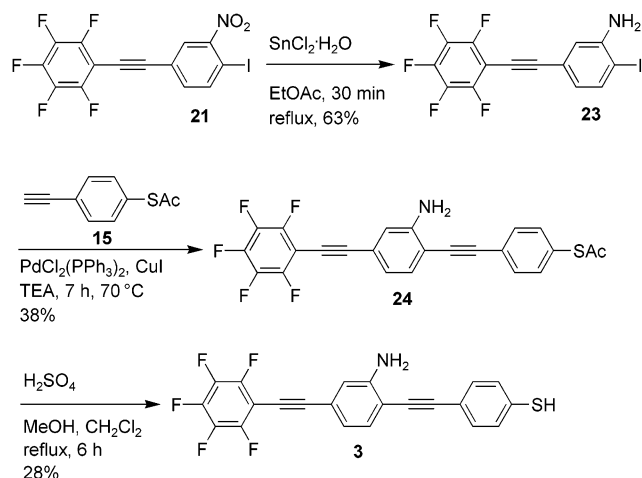
(26) Kosynkin, D. V.; Tour, J. M. *Org. Lett.* **2001**, *3*, 991.

(27) Under the typical deprotection condition of the TMS-acetylene (i.e., dissolved in $CH_2Cl_2/MeOH$ and treatment with K_2CO_3), 4-methoxy-2,3,5,6-tetrafluorophenylethyne was isolated as a white solid.

Scheme 2



Scheme 3



extended aniline **28**, compared to the approach used to prepare the regioisomeric intermediate **20** (Scheme 2). Subsequent iodination was performed under the same diazotization and iodination conditions as previously used, to isolate **29**. Final coupling with the alligator clip **15** and deprotection of the resulting thioacetate yielded the mono-nitro OPE **4** as the free thiol.

Having the regioisomeric intermediates **21** and **29** in hand, it was convenient to couple them with other alligator clips to afford OPEs capable of forming molecule–metal junctions.

Scheme 5 depicts the synthesis of two OPEs with nitrile alligator clips and two OPEs with pyridyl alligator clips, by coupling the iodides **21** and **29** with the corresponding 4-ethynylbenzonitrile **31**¹⁴ and 4-ethynylpyridine **32**,²⁸ affording the desired final OPEs **5–8**. As illustrated in Scheme 6, a third pyridyl-containing OPE **9** with both amine and

nitro functional groups was synthesized. The presence of electron-rich and electron-deficient groups in the same π ring might favor close cofacial π -stacking.²⁹

To synthesize **9**, free alkyne **26** was coupled with the dibromide **33**,²⁵ yielding **34**. Further TMSA-coupling to the remaining bromide afforded **35** and subsequent deprotection of the corresponding alkyne afforded **36**. A final coupling with 4-iodopyridine **37**¹⁵ resulted in the desired pyridine-containing OPE **9**.

Having the free alkyne **36** in hand, we attempted to prepare a free thiol target, as depicted in Scheme 7. Alligator clip **38** was coupled in a Sonogashira reaction, affording **39**. However, when attempting deprotection of the thioacetate under acidic conditions, the material was too unstable to allow its isolation.³⁰

2.3. Thermal Analysis. Several solution-phase preparations of SAMs for molecular electronics have been developed, and related recent techniques have focused on the deposition of organic thin films,³¹ with a desire toward formation of cleaner intact films of oligomers⁵ and polymers with low⁶ and average molecular weight.³² Gas-phase deposition could be particularly interesting since no solvents are present to coadsorb on the substrate, and our initial use of vapor-phase depositions, under ambient pressure conditions, have led to more uniform and well-ordered SAMs.³³ The use of inert and UHV atmospheres (ca. 10^{-10} Torr)

(29) Warner, M. *Crystal Structure Determination*; Teubner: Stuttgart, 1996.

(30) **CAUTION!** Deprotection of compound **39** on a 4-mmol scale resulted in a violent explosion, which caused permanent damage to surrounding laboratory items. See the Experimental Section and Tour, J. M.; Lamba, J. S. *J. Am. Chem. Soc.* **1993**, *115*, 4935.

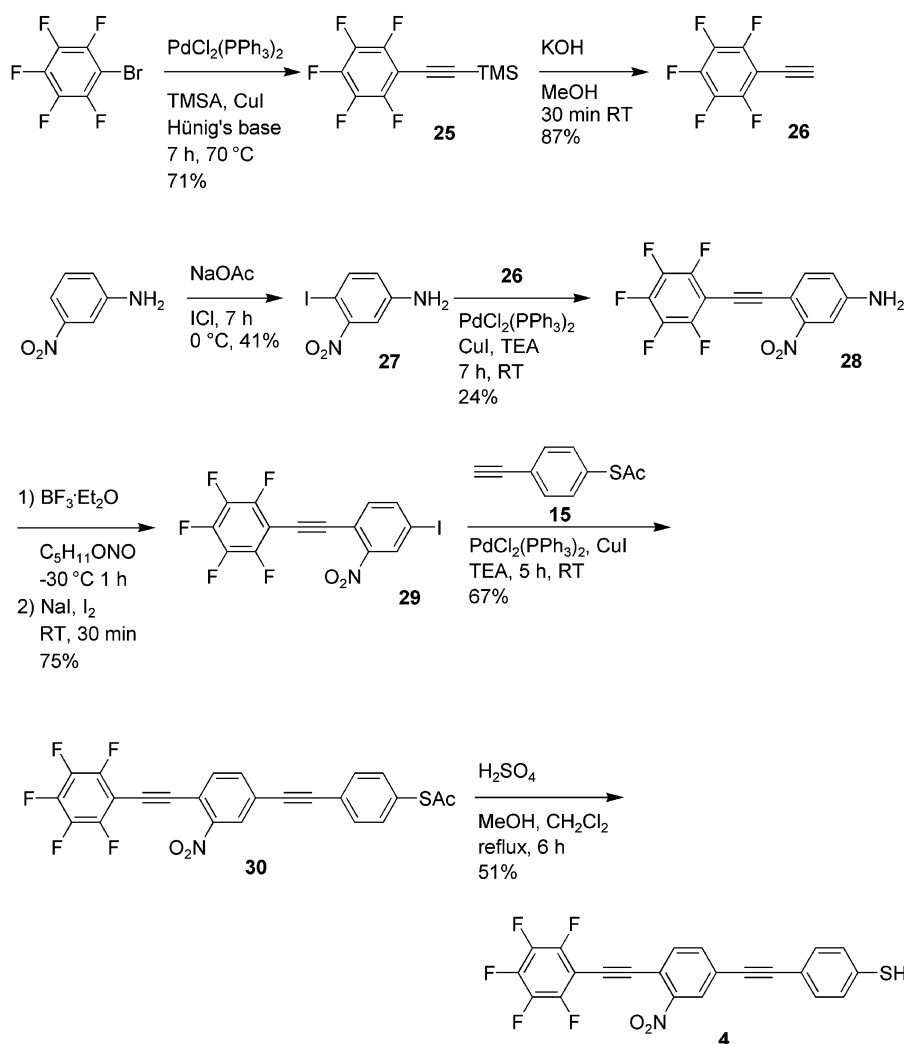
(31) Pique, A.; McGill, R. W.; Chung, R.; Bucaro, M. A. *Thin Film Solids* **1999**, *536*, 355.

(32) Bubb, D. M.; Ringeisen, B. R.; Callahan, J. H.; Galicia, M.; Vertes, A.; Horwitz, J. S.; McGill, R. A.; Houser, E. J.; Wu, P. K.; Pique, A.; Chrisey, D. B. *Appl. Phys. A* **2001**, *73*, 121.

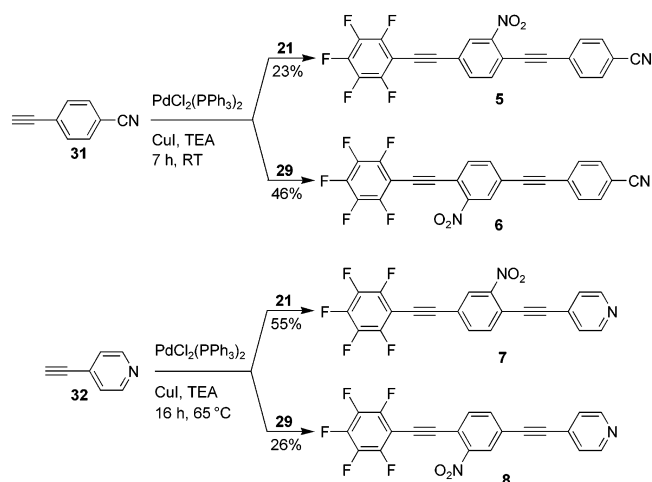
(33) Donhauser, Z. J.; Price D. W., Jr.; Tour, J. M.; Weiss P. S. *J. Am. Chem. Soc.* **2003**, *125*, 11462.

(28) Ziessel, R.; Suffert, J. *Tetrahedron Lett.* **1991**, *32*, 757.

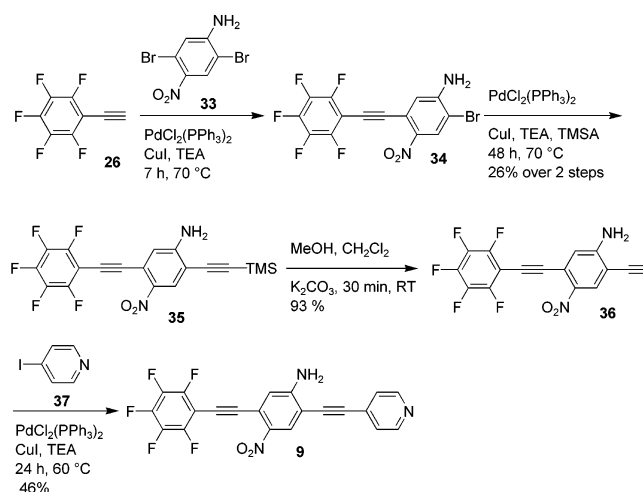
Scheme 4



Scheme 5



Scheme 6



should allow molecular components to evaporate at lower temperatures,³⁴ preserving the original integrity of the molecular components, while being compatible with state-of-the-art PVD fabrication processes.

With this view in mind, we explored the thermal stability of our fluorinated OPEs as candidates for vapor phase

assembly and compared these to the nonfluorinated analogues. DSC can provide an indication of the melting point, noted by a sharp endothermic transition, and decomposition temperature of molecular systems, represented by an exothermic transition. Often a sharp exotherm is related to an intramolecular event, whereas a broad exotherm is indicative of cross-linking.³⁵ Figures 4 and 5 show the DSC thermograms for compounds **6** and **7**, respectively, wherein there

(34) A gas chromatography analysis showed that a small amount of compound **1** sublimed at 150°C under a pressure of 0.05 mmHg.

Scheme 7

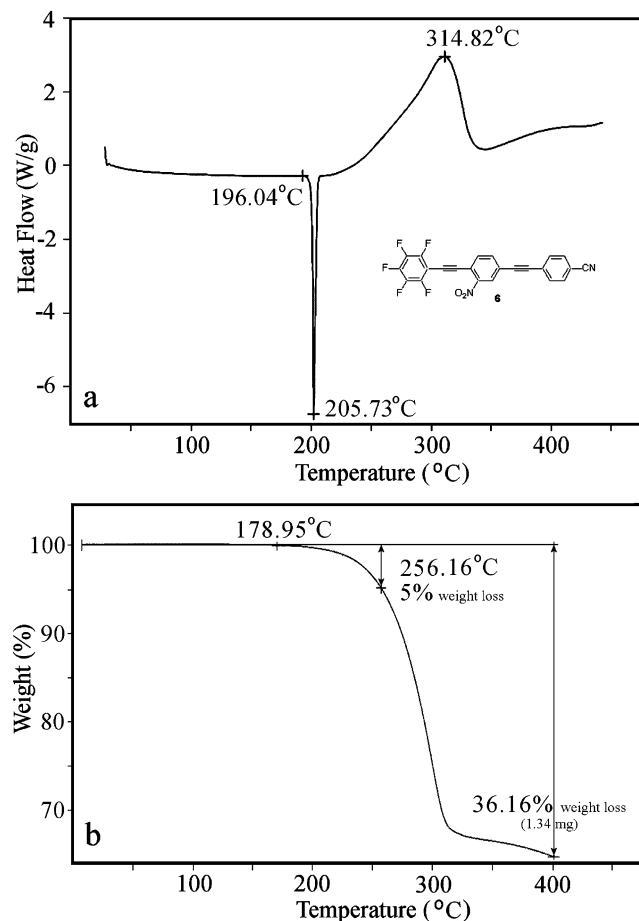
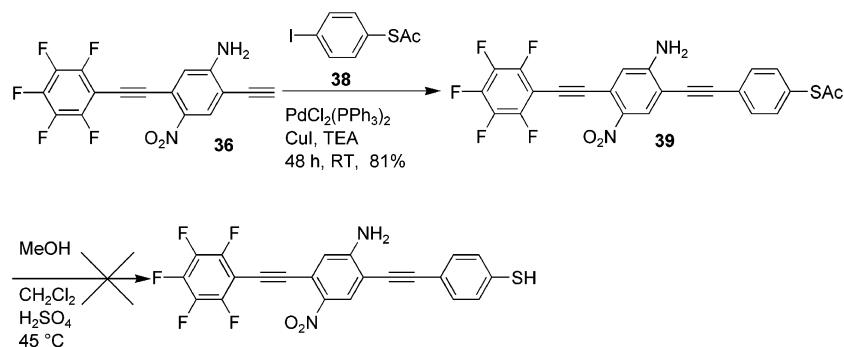


Figure 4. (a) DSC profile for OPE **6**, showing an endotherm (melting point) with its lowest point at 205°C , followed by an exotherm (decomposition) reaching a maximum of 315°C . (b) TGA profile of the same compound, showing ca. 36% weight loss over a range of 400°C .

are sharp endothermic events (melting) at 206 and 177°C , respectively, followed by broad decomposition (cross-linking) events.

DSC could provide a pre-screen for use of these compounds in vapor deposition device assemblies. Thermogravimetric analysis (TGA), which is usually performed at standard pressure, shows the temperature at which molecular components evolve from a sample. As expected, the results (Table 1) showed a common pattern in that the decomposition temperatures were 30 – 50°C higher in the fluorinated versions.³⁶ Note that the thiols were not tested because of

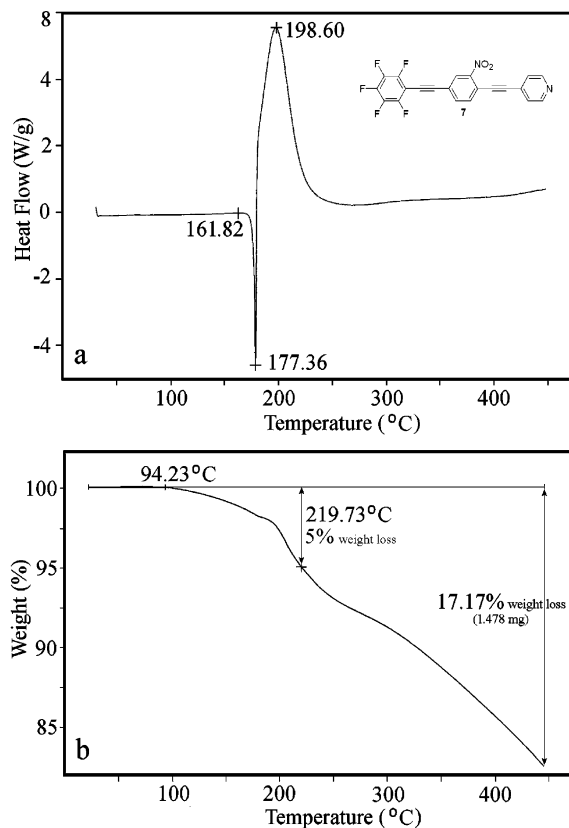


Figure 5. (a) DSC profile for OPE **7**, showing an endotherm (melting point) peaking at 177°C , followed by an exotherm reaching a maximum of 199°C . (b) TGA profile of the same compound, showing a 17% weight loss over a range of 450°C .

their oxidative instability and risk of reaction with the thermal analysis pans. Therefore, the fluorinated versions described here are more thermally stable than their nonfluorinated analogues, and they would be more amenable to PVD formation of organic assemblies in UHV.

2.4. Monolayer Formation Analysis. The chemical integrity at the chemical interface level of the SAMs was initially verified by single-wavelength ellipsometry (SWE), contact angle, and cyclic voltammetry (CV).

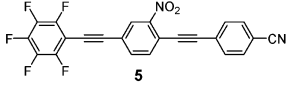
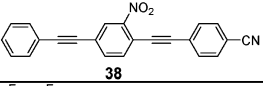
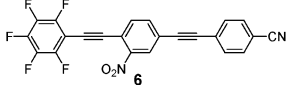
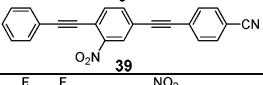
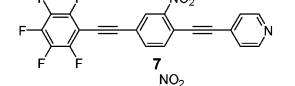
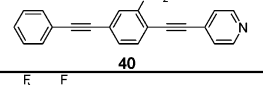
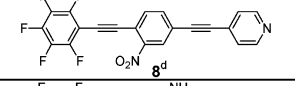
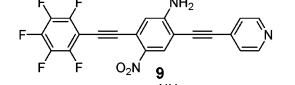
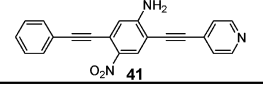
Multiple ellipsometric measurements at different spots on several different samples for each type of SAM were

(35) Stevens, M. P. *Polymer Chemistry, An Introduction*; Oxford University Press: New York, 1999.

(36) Schultz, J.; Bhatt, J.; Chartoff, R. P.; Pogue, R. T.; Ullett, J. S. *J. Polym. Sci. B* **1998**, *37*, 1183.

(37) Chanteau, S. H. *Synthesis of Conjugated Molecules: From Electronics to Molecular ART*, Ph.D. Thesis, Rice University, Houston, TX, 2003, p 41.

Table 1. Thermal Comparison of Fluorinated OPEs vs Non-fluorinated OPEs (Compounds 38,¹⁴ 39,¹⁴ 40,¹⁵ and 41³⁷ were Included for Comparison)

Compound	Melting Point ^a (°C)	Decomposition ^b (°C)
 5	NO ^c	160
 38	NO ^c	125
 6	206	210
 39	136	140
 7	177	180
 40	136	140
 8 ^d	176	180
 9	NO ^c	220
 41	101	188

^a Recorded by a sharp endotherm in DSC; recorded at peak. ^b Recorded by a large exotherm in DSC; recorded at onset. ^c No melting point was observed by DSC. ^d Nonfluorinated version was not synthesized for comparison.

collected, and the resulted average experimental thickness is compared with the theoretical thickness in Table 2. The comparison also includes static (Θ_{stat}) water contact angles for every SAM and hexadecane (HD) contact angles for SAMs from 2 and 3. The water contact angles for the SAMs made from the pyridines 7–9 are slightly higher than the values for a SAM prepared with an analogous nonfluorinated compound 10.^{38,39} The change in hydrophobicity may indicate a SAM with fewer defects.⁴⁰ The very low HD contact angles indicate that SAMs 2 and 3 are disordered.^{40a} Except for the nitriles 5 and 6,⁴¹ the rest of the compounds achieved a close (but not full) SAM formation within 24 h.

Compared with our recent work with analogous nonfluorinated compounds such as 10,³⁸ the experimental thicknesses values reported in Table 2 may indicate lower order in the SAM formation, despite literature that indicates

Table 2. Comparison of Theoretical and Experimental Thicknesses, and Static Contact Angle Goniometry (Θ_{stat}) of SAMs Made of Compounds 1–9

entry	compound	SWE ^a (Å)		Θ_{stat} ^d	
		theoretical ^b	experimental	H ₂ O	HD
1	1-SAM ^e	21	16	90.7	
2	2-SAM ^e	21	17	87.7	10
3	3-SAM ^e	21	14	89.2	0
4	4-SAM ^{f,g}	20	15	93.6	
5	5-SAM ^g	20 ^c	13	85.6	
6	6-SAM ^g	20 ^c	13	83.9	
7	7-SAM ^g	18	16	88.9	
8	8-SAM ^g	18	15	85.8	
9	9-SAM ^g	18	14	90.3	

^a Within $\pm 10\%$ of error. ^b At 20° to surface normal angle. ^c Pt–N bond length taken as 1.13 Å. ^d $\pm 3^\circ$. ^e SAMs on Au. ^f Using CH₂Cl₂ as solvent for SAM formation, see ref 39. ^g SAMs on Pt.

otherwise.¹⁹ However, the tilt angle may be $>20^\circ$ from the surface normal, therefore bringing the experimental data more in concert with the calculated thicknesses. Also, longer reaction times and more suitable solvents may allow for the formation of full and closer-packing SAMs. The measured film thicknesses averaged about 70% of the theoretical values.

Additional characterization of the average compactness and extent of structural defects of SAMs on electrodes was determined by CV following a previously reported technique.⁴² Comparison of redox currents of an electroactive species, for example ferricyanide [$\text{Fe}^{\text{III}}(\text{CN})_6^{3-}$] used in this study, on bare electrodes and on electrodes coated with SAMs, gives a good indication of the surface coverages of the SAMs. Due to the passivation effect from the molecular monolayer, decreased redox currents are expected on the SAMs-coated electrodes. Figure 6 shows CVs of bare electrodes and electrodes self-assembled with compounds 1, 4, and 5, in solutions of 1 mM K₃[Fe(CN)₆] and 0.1 M KCl.

The CVs show a good current passivation by SAMs of the adsorbates 1 on Au and 4 on Pt electrodes, whereas the assembly of compound 5 on Au electrode indicated partial passivation. In all cases the SAMs at least partially inhibited transport of the active ion ferricyanide to the metal surface under the CV conditions.⁴³ The CV results support our previous observations for similar oligomers.^{38,44}

2.5. Chemical Interface Analysis. A closer examination of the chemical composition of the SAM was pursued with a series of XPS experiments. Figure 7 summarizes high-resolution XPS multiplets for the C1s region of SAMs on Au prepared with compounds 1–4.

The signal is clearly made of two different peaks. The main component, the nonfluorinated carbons from the aromatic ring, lies at the binding energy of ca. 284.5 eV (Figure 7, light blue peak), while the higher energy of the second peak is characteristic of the more electron-deficient fluorinated aromatic ring (Figure 7, dark blue peak).

The split of the carbon signal into two well-defined peaks, their relative ratios, and their binding energies, were con-

- (38) Stapleton, J. J.; Harder, P.; Daniel, T. A.; Reinard, M. D.; Yao, Y.; Price, D. W.; Tour, J. M.; Allara, D. L. *Langmuir* **2003**, *19*, 8245.
 (39) Furthermore, we found that the contact angle of a SAM made of 4 can be increased from 85.1° to 93.6° by changing EtOH/CH₃CN to CH₂Cl₂ as a solvent during the SAM preparation.
 (40) (a) Bain, C. D.; Troughton, E. B.; Tao, Y.-T.; Evall, J.; Whitesides, G. M.; Nuzzo, R. G. *J. Am. Chem. Soc.* **1989**, *111*, 321. (b) Bain, C. D.; Evall, J.; Whitesides, G. M. *J. Am. Chem. Soc.* **1989**, *111*, 7155. (c) Zehner, R. W.; Sita, L. R. *Langmuir* **1997**, *13*, 2973.
 (41) A dominance of a η^2 - (i.e., π - or side-on) over a η^1 -coordination (or σ -bonding via the N) through the triple bond and the surface, could be responsible for lower SAM thicknesses using compounds 5 and 6; see Steiner, U. B.; Caseri, W. R.; Suter, U. W. *Langmuir* **1992**, *8*, 2771.

- (42) Cheng, L.; Yang, J.; Yao, Y.; Price, D. W., Jr.; Dirk, S. M.; Tour, J. M. *Langmuir* **2004**, *20*, 1335.
 (43) Fan, F.-R.; Yao, Y.; Cai, L.; Cheng, L.; Tour, J. M.; Bard, A. J. *J. Am. Chem. Soc.* **2004**, *124*, 4035.
 (44) Maya, F.; Flatt, A. K.; Stewart, M. P.; Shen, D. E.; Tour, J. M. *Chem. Mater.* **2004**, *16*, 2987.

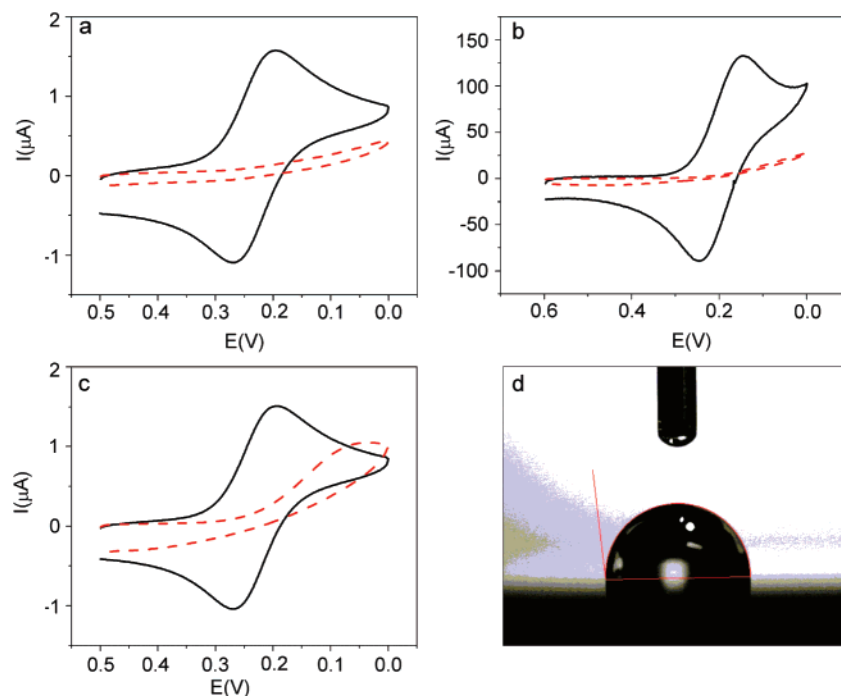


Figure 6. Cyclic voltammograms in a solution of 1 mM $\text{K}_3[\text{Fe}(\text{CN})_6]$ and 0.1 M KCl on bare electrodes (solid lines) and SAM-coated electrodes (curved lines): (a) compound **1** on Au, (b) compound **4** on Pt, and (c) compound **5** on Au. Potentials were reported vs a silver/silver chloride reference electrode (Ag|AgCl) in plots (a) and (c), but a saturated calomel reference electrode (SCE) in plot (b). Scan rate was 0.1 V/s at an initial negative scan direction. The Au disk electrodes used for plots (a) and (c) have a diameter of 1 mm, whereas the Pt electrode has a diameter of 9 mm. (d) Contact angle profile of a 20- μL drop of water on SAM of **4** on Pt.

sistent in all the cases and with our previous XPS analyses of similar fluorinated oligomers.^{44,45} Deconvolution of the carbon signal allowed the elucidation of a third component at ca. 285.7 eV for every SAM (Figure 7, pink peak). For the carbon region, the ratio of this third peak relative to the other two peaks varies on every SAM, having a direct relationship to the number of carbons adjacent to electron-deficient carbons bearing electronegative atoms (as F, and N for the $-\text{NO}_2$ and $-\text{NH}_2$ functional groups).

The third type of carbon includes the C–S carbon (Figure 7, pink peak) from the alligator clip. Using this correlation, the theoretical ratio for the three carbon peaks of SAM-**1** is (fluorinated carbon/adjacent carbons/nonfluorinated carbons) 5:2:15, while the deconvolution in Figure 7 for the three carbon peaks on the same SAM gives an experimental ratio of 5:1.8:15. The similarity of the theoretical to the experimental ratios of the three carbon types for all SAMs is evidence for the integrity of the molecular thin film on the surface. Furthermore, XPS survey spectra (not shown) for all the SAMs showed the absence of chemical elements that were not part of the oligomers. Although these analyses are for SAMs formed in solution, we can capitalize on the high thermal stability of the fluorinated oligomers for their use in PVD processes, expecting to observe a good chemisorption of the oligomers as we have seen with vapor phase annealing of alkanethiolate SAMs.³³ High-resolution XPS multiplex for the N and S region were also acquired for SAMs made of compounds **1–4** as shown in Figure 8, while the signals for the N region on SAMs made of the pyridines **7–9** are

collected in Figure 9. Table 3 summarizes the binding energies, the relative concentrations of the SAMs, and the chemical species of interest.

From Figure 8, it is worth noting the second signal on SAM-**2** for the N1s region, assigned to an aromatic amine group, from a SAM made with the compound **22** (the thioacetyl-protected precursor of compound **2**) that has no other functional group on its central ring but a nitro. The presence of the amine originates from the reduction of the nitro group when the oligomer **22** was assembled under basic conditions, as shown previously.³⁸ The S2p signal (Figure 8, right side) contained a doublet centered at ca. 163 eV corresponding to the S covalently attached to the Au surface. When compared with previous work,⁴⁴ S chemisorbed on Au was the main component in the S region for all SAMs, observing little or no signal for unreacted thioacetate or thiol. Figure 9 shows the N region from SAMs formed with pyridines **7–9**, with a main signal at ca. 400 eV, corresponding to the pyridyl N.⁴⁶ In case of compound **9** as chemisorbate, the signals from the pyridyl and the amino groups coincide. For all the SAMs, a small component with a higher binding energy of 405.6 eV is assigned to the nitro group (Figure 9 and Table 3). On the basis of results shown in Figures 8 and 9, we observed that free thiols (and not the thioacetyl-protected versions) such as **2** allowed for direct assembly on Au, with no need for the deprotection step, and more importantly, the integrity of the adsorbed organic film was maintained.⁴⁷

To complement our analyses at the chemical interface, FTIR analysis was done to gain more data on the physical characteristics of the adsorbed organic films. Figure 10 shows

(45) Stewart, M. P.; Maya, F.; Kosynkin, D. V.; Dirk, S. M.; Stapleton, J. J.; McGuiness, C. L.; Allara, D. L.; Tour, J. M. *J. Am. Chem. Soc.*, **2004**, *126*, 370.

(46) Ng, S. S.; Chan, H. S. O.; Lu, G.-F. *Macromolecules* **2003**, *36*, 1543.

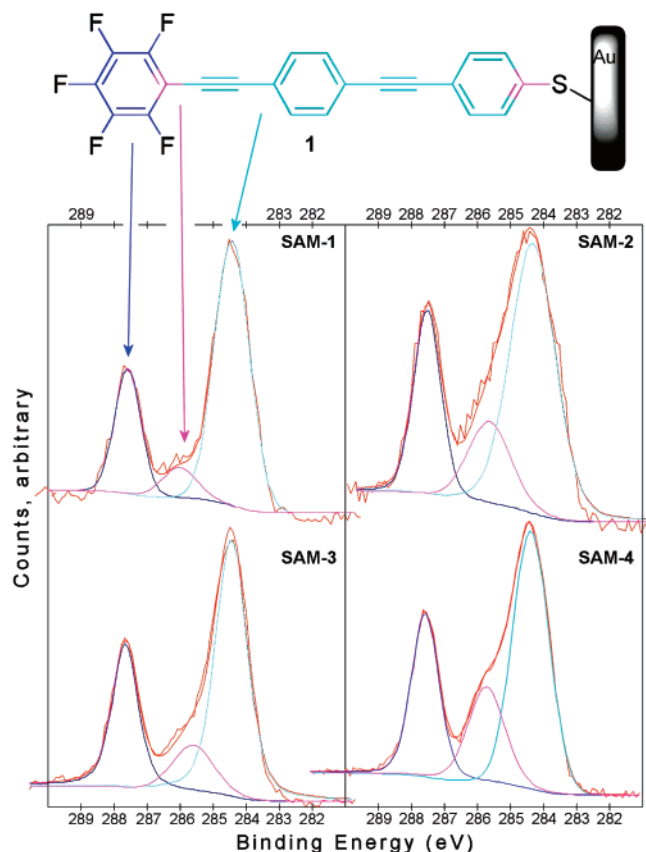


Figure 7. High-resolution XPS multiplex for the C1s region of SAMs on Au of compounds 1–4. In all four SAMs, two main components at ca. 284.5 eV (right peak in light blue) and 287.7 eV (left peak, dark blue) correspond to the nonfluorinated and fluorinated Cs respectively; while a third component (pink) is evident only after deconvolution. The chemical structure of chemisorbed 1 shows the assignment of the three peaks to the different carbons (nonfluorinated carbons, light blue; fluorinated carbons, dark blue; and adjacent carbons, pink) from the molecular backbone. XPS pass energy was 11.75 eV in a 45° takeoff angle. The Au 4f_{7/2} binding energy of 84.00 eV was taken as a reference for all SAMs.

the spectrum of a grazing-angle FTIR experiment (inset a), with the structural features related to the chemisorbed 4 on Pt, providing information about its intact presence on the surface. Comparable features are present in both the IR absorption of SAM-4 (Figure 10a) and the KBr pellet spectrum of the compound 4 (Figure 10b).

A weak aromatic stretching band $\nu_{\text{as}}(\text{C-H})$ is present at 3083 cm⁻¹ for the KBr pellet spectrum (Figure 10b), as well as a moderately weak S-H mode $\nu_{\text{as}}(\text{SH})$ at 2562 cm⁻¹. A weak band at 2209 cm⁻¹ in the KBr pellet spectrum (Figure 10b) represents the absorption of the triple bond, which is also seen with a very weak intensity in the grazing-angle spectrum (Figure 10a). Plane ring breathing $\nu(\text{C=C})$ modes at 1548 and 1499 cm⁻¹ can be seen in the SAM on Pt (Figure 10a), absorbing near the antisymmetric NO₂ stretch $\nu_{\text{as}}(\text{NO}_2)$ mode at 1526 cm⁻¹ and the symmetric NO₂ stretch $\nu_{\text{s}}(\text{NO}_2)$ mode at 1445 cm⁻¹. At lower wavenumbers, an in-plane aromatic C-H deformation $\nu_{\text{ip}}(\text{C-H})$ mode at 996 cm⁻¹ is

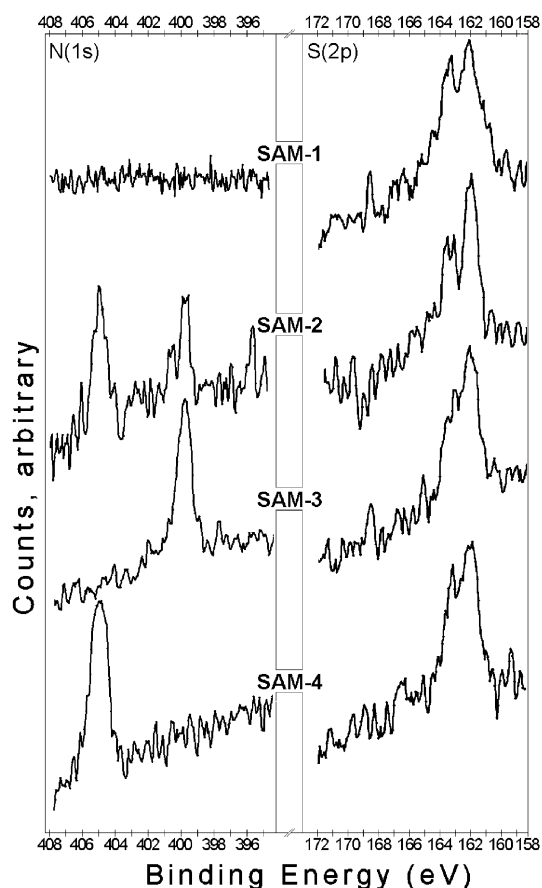


Figure 8. High-resolution XPS multiplex for the N1s and S2p regions (left and right columns, respectively) of SAMs on Au of compounds 1–4 after a 24 h assembly time; the N region of SAM-1 was included for comparison. For the SAM-2, note the presence of two peaks assigned to nitro and amine groups in a ca. 1:1 ratio. XPS pass energy was 11.75 eV at a 60° takeoff angle. The Au 4f_{7/2} binding energy of 84.00 eV was taken as a reference for all SAMs.

present in both spectra of Figure 10, as well as an out-of-plane aromatic C-H deformation $\nu_{\text{op}}(\text{C-H})$ mode at 923 cm⁻¹ with a weak intensity.

Combined with the surface analysis data, this comparison of FTIR spectra provides clear evidence for the integrity of organic films made from electron-deficient fluorinated OPEs.

3. Summary

We present the synthesis of new OPEs that contain a polyfluorophenyl ring and various alligator clips, including pyridines, nitriles, or free thiols, with no need for further deprotection to achieve chemisorption. Calculations at the DFT level indicate that the pentafluoro aromatic ring produces a strong dipolar moment directed away from the alligator clip. The synthetic design of OPEs 1–9 includes redox centers, features that have been found to be important in prior work from this lab.² Thermal analysis by DSC and TGA showed higher thermal stability for the fluorinated OPEs. Goniometry, IR, and X-ray photoelectron spectroscopy confirm the ability of these new fluorinated oligomers, synthesized as free thiols, to form SAMs on Au and Pt surfaces. From these experimental and theoretical results, it is logical that fluorinated OPEs would be good candidates for SAM formation processes using PVD. The electrical and

(47) The comparison of the XPS signals at the N1s region from a SAM made of 22 and a SAM made of 2, as well as signals from SAMs made of pyridines 7–9, allowed us to confirm that the reduction of the nitro group was not the result of a chemical degradation caused by the emission of the electrons upon X-ray excitation during the XPS analysis.

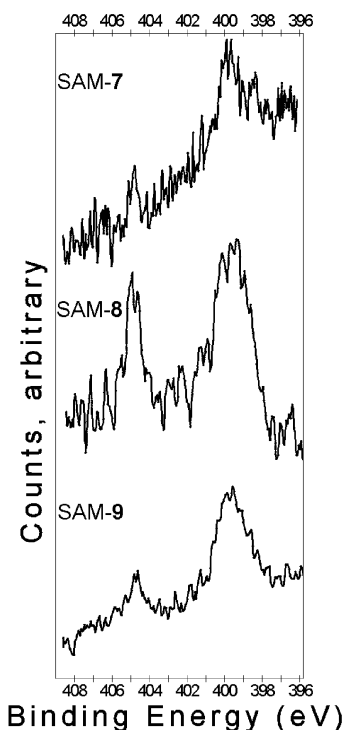


Figure 9. High-resolution XPS multiplex for the N1s region of SAMs made with compounds 7–9 on Pt for 24 h. XPS pass energy was 11.75 eV in a 60° takeoff angle. The Pt 4f_{7/2} binding energy of 71.00 eV was taken as a reference for all SAMs.

thermal testing of these targets for further fabrication of molecular-based architectures is a work in progress.

4. Experimental Section

4.1. Thermal Analyses. TGA was performed in a TA Q₅₀ TGA7 30–400 °C or 30–800 °C at 10 °C/min under N₂ gas. For experiments heating to 400 °C, aluminum pans were used, whereas for experiments at higher temperatures, platinum pans were used. DSC was performed with a TA Q₁₀ using a 30–450 °C scanning window at 10 °C/min under N₂ gas.

4.2. Gold Substrates. Gold films were deposited by thermal evaporation of a 200-nm-thick Au layer onto Si wafers with a 25-nm Cr adhesion layer at a rate of 1 Å/s at 2 × 10^{−6} Torr. Before use, the Au substrates were cleaned by a UV/O₃ cleaner (Boekel Industries, Inc., model 135500) for 10 min to remove organic contamination, and submerged in ethanol for 10 min before being dried in flowing N₂. This procedure was used to provide a reproducibly clean Au surface.^{48,49} The Pt substrates for FTIR measurements were prepared and provided by Z. Li of Hewlett-Packard laboratories, Palo Alto, CA.

4.3. Self-Assembly. The oligomer as free thiol (1 mg) was dissolved in the corresponding solvent (3–4 mL). Unless otherwise stated, the cleaned substrates (Au or Pt) were immersed into the adsorbate solution at room temperature for a period of 24 h, followed by 5 h at 40 °C to promote closer molecular packing, the same methodology used in our previous work.^{33,34} All the solutions were freshly prepared, previously purged with N₂ for an oxygen-free environment, and kept in the dark during immersion to avoid photooxidation. After assembly, the samples were removed from the solution, rinsed thoroughly with EtOH then acetone, and blown dry with N₂.

4.4. SWE Measurements. Measurements of surface optical constants and molecular layer thicknesses were taken with a single-wavelength (632.8 nm laser) Gaertner Stokes ellipsometer. The n_s and k_s values were the result of several measurements recorded for every clean substrate and used for their corresponding SAM-adsorbed sample. The refractive index was $n_f = 1.55$ for all compounds ($k_f = 0$).⁵⁰

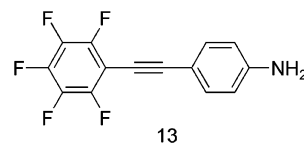
4.5. Contact Angle Goniometry. Static contact angle was measured using a Rame-Hart 2001 apparatus. A 20-μL drop of ultrapure water was dispensed onto the surface using a flat-tipped micrometer syringe. Images of the drop were captured digitally using a CCD camera, and contact angles were analyzed using the RHI 2001 software.

4.6. CV-Monitored Electrode Passivation. The electrochemistry experiments were carried out using a BAS CV-50W voltammetric analyzer (Bioanalytical Systems, Inc). A conventional three-electrode cell was used with a Au or Pt substrate as the working electrode with surface area of 1 cm², with a Pt wire as the counter electrode, and a Ag/AgNO₃ (10 mM AgNO₃ and 0.1 M Bu₄NBF₄ in acetonitrile) as the reference electrode. The scan rate was 0.1 V/s at 23 °C with an initial scan direction that was negative. Self-assembly on the working electrode was performed in an organic solution of 1 mM of the corresponding oligomer.

4.7. XPS Measurements. A Physical Electronics (PHI 5700) XPS/ESCA system at 3 × 10^{−9} Torr was used for photoelectron spectra acquisition. A monochromatic Al X-ray source at 350 W was used with an analytical spot size of 800 μm. Takeoff angles of 60 and 45° were used, with a pass energy of 11.75 eV. The Au 4f_{7/2} binding energy of 84.00 eV and the Pt 4f_{7/2} binding energy of 71.00 eV were taken as references.

4.8. Calculations. Total energies, dipole moments, and HOMO/LUMO energies were calculated using Spartan 5.1.⁵¹ The oligomers' structures were geometry minimized at the modified neglect of diatomic overlap (MNDO) level previous to an optimization at the density functional theory (DFT) level.

4.9. FTIR Measurements. A Nicolet Nexus 860 FTIR bench with an MCT/A detector, and SMART SAGA grazing angle accessory (Thermo Electron) fixed at 80° angle of incidence, were used to measure infrared spectra from an organic layer on Pt. Samples used a plasma-cleaned Pt wafer as background. Sample spectra were averaged over 1000 scans at 2 cm^{−1} resolution.



4.10. 4-Pentafluorophenylethynylphenylamine (13). Following the Sonogashira coupling protocol, bromopentafluorobenzene (19.0 g, 77.0 mmol), 4-ethynylaniline **12**²³ (9.0 g, 77.0 mmol), PdCl₂(PPh₃)₂ (2.7 g, 3.8 mmol), and CuI (1.5 g, 7.7 mmol) were dissolved in THF (150 mL). Hünig's base (54.0 mL, 307.0 mmol) was added and the reaction was stirred overnight at 70 °C. Purification by flash chromatography (CH₂Cl₂) afforded the desired product (4.4 g, 21% yield) as a dark yellow solid; mp 133–137 °C. IR (KBr) 3483, 3394, 2605, 2566, 2208, 1610, 1522, 1445, 1291, 1176 cm^{−1}. ¹H NMR (400 MHz, CDCl₃) δ 7.38 (m, 2H), 6.65 (m, 2H), 3.93

(48) Ron, H.; Matlis, S.; Rubinstein, I. *Langmuir* **1998**, *14*, 1116.

(49) Ron, H.; Rubinstein, I. *J. Am. Chem. Soc.* **1998**, *120*, 8486

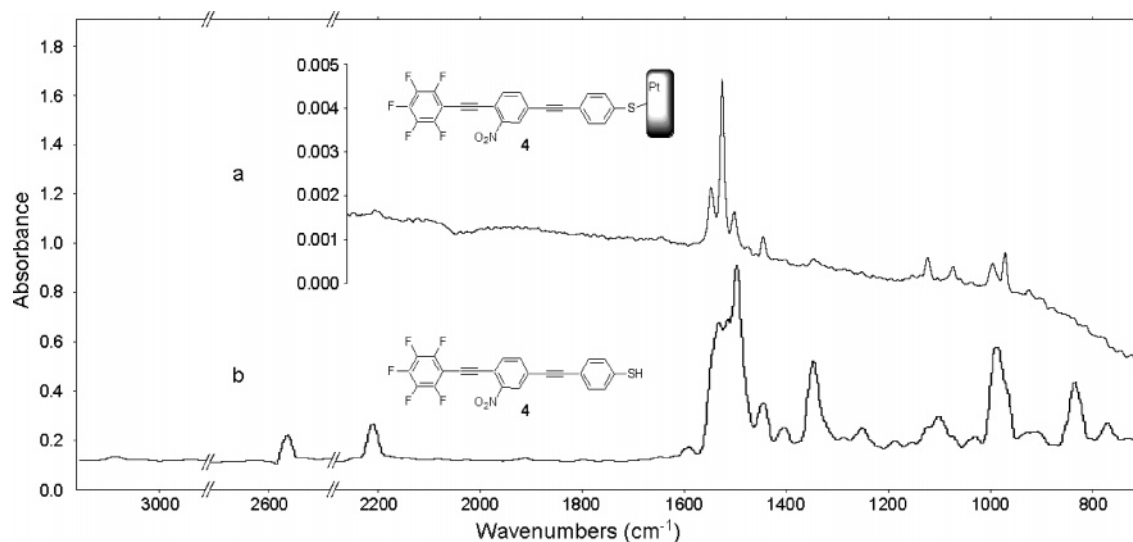
(50) Tour, J. M.; Jones, L.; Pearson, D. L.; Lamba, J. S.; Burgin, T. P.; Whitesides, G. W.; Allara, D. L.; Parikh, A. N.; Atre, S. V. *J. Am. Chem. Soc.* **1995**, *117*, 9529.

(51) *Spartan version 5.1*; Wavefunction, Inc., 18401 Von Karman Avenue, Suite 370, Irvine, CA 92612.

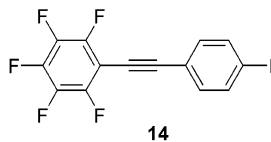
Table 3. Binding Energies and Relative Concentrations for the Chemical Species of Interest, Observed by XPS on SAMs Formed with Compounds 1–9^a

compound	binding energy (eV) ^b				relative concentration (%) ^c			
	F(1s)	N(1s)	C(1s)	S(2p ^{1/2})	F(1s)	N(1s)	C(1s)	S(2p)
1–SAM ^d	687.98		287.58 286.05 284.41	162.05	17.35		51.48	4.18
2–SAM ^{d,e}	688.17	405.70 400.00	287.85 286.20 284.64	162.01	21.79	4.51	49.64	2.48
3–SAM ^d	687.86	399.17	287.49 285.70 284.28	162.12	19.42	3.55	52.09	2.09
4–SAM ^f	687.93	405.60	287.55 285.43 284.37	162.23	19.61	4.33	49.71	3.21
5–SAM ^d	688.26	405.65 399.41	288.21 285.93 284.43		4.43	8.40	34.99	
6–SAM ^d	687.92	405.68 399.46	287.52 285.97 284.36		4.09	5.36	39.48	
7–SAM ^g	688.36	405.84 398.99	287.99 285.43 284.37		8.48	5.92	38.90	
8–SAM ^g	688.31	405.82 399.70	287.96 285.81 284.48		4.91	4.32	43.29	
9–SAM ^g	688.20	405.76 399.41	287.77 285.66 284.42		9.06	8.17	43.84	

^a SAM formation was promoted in THF/EtOH or CH₂Cl₂ as solvents for 24 h at room temperature, plus 4 h at 40 °C. When a thioacetyl-protected compound was used, an initial incubation with NH₄OH for 10 min was needed; see ref 43. The Au 4f_{7/2} binding energy of 84.00 eV and the Pt 4f_{7/2} binding energy of 71.00 eV were taken as references. ^b Values with ±0.2 eV of error. ^c Values with ±2% of error; for entries 1–4 Au comprises the remainder of the measured elements, while for entries 5–9 Pt comprises the remainder of the measured elements. ^d THF/EtOH 1:1 used as solvent for SAM formation. ^e Thioacetyl-protected compound 22 used and deprotected in situ with NH₄OH; see ref 43. ^f CH₂Cl₂ used as solvent for SAM formation. ^g THF used as solvent for SAM formation.

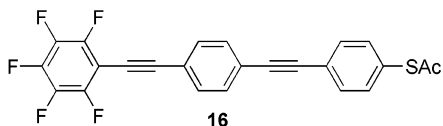
**Figure 10.** Comparison of (a) a grazing angle spectrum of a SAM made of compound 4 on platinum, with (b) a KBr pellet absorption of the same compound as a free thiol.

(br s, 2H). ¹³C NMR (100 MHz, CDCl₃) δ 148, 133.6, 114.8, 110.8, 103, 101.4, 71.4. HRMS calcd for C₁₄H₆F₅N, 283.0420; found, 283.0423.

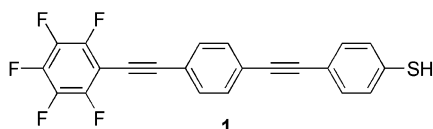


4.11. 4-Pentafluorophenylethynyl iodobenzene (14). Following the general iodination procedure via diazotization, **13** (4.3 g, 15.2

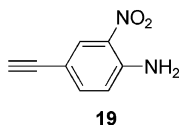
mmol) dissolved in THF (20 mL) was added to BF₃·Et₂O (7.7 mL, 60.8 mmol) followed by the addition of isoamyl nitrite (7.1 mL, 53.2 mmol). After the precipitate was isolated, it was added to a solution of NaI (2.4 g, 16.2 mmol) and I₂ (3.1 g, 12.1 mmol) in CH₃CN (20 mL). Purification by flash chromatography (3:1, hexanes/CH₂Cl₂) afforded the desired product (2.1 g, 35% yield) as a white solid; mp 121–125 °C. IR (KBr) 3016, 2621, 2485, 2434, 2216, 1918, 1713, 1498, 1438, 1367, 1223, 1113 cm⁻¹. ¹H NMR (400 MHz, CDCl₃) δ 7.75 (m, 2H), 7.29 (m, 2H). ¹³C NMR (100 MHz, CDCl₃) δ 137.9, 133.4, 121.1, 109.7, 99, 96.2. HRMS calcd for C₁₄H₄F₅I, 393.9278; found, 393.9287.



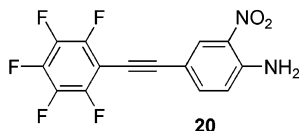
4.12. Thioacetic acid 4-(4-pentafluorophenylethynylphenylethynyl)phenyl ester (16). Following the Sonogashira coupling protocol, **14** (520 mg, 1.4 mmol), **15**²⁵ (244 mg, 1.4 mmol), PdCl₂(PPh₃)₂ (93 mg, 0.14 mmol), and CuI (51 mg, 0.28 mmol) were dissolved in THF (20 mL). TEA (0.7 mL, 5.2 mmol) was added and the reaction was stirred at room temperature overnight. Purification by flash chromatography (1:1, hexanes/CH₂Cl₂) afforded the desired product (290 mg, 47% yield) as a yellow solid; mp 199–203 °C. IR (KBr) 3040, 2912, 2485, 2423, 2210, 1910, 1712, 1516, 1494, 1443, 1355, 1114 cm⁻¹. ¹H NMR (400 MHz, CDCl₃) δ 7.57 (m, 6H), 7.44 (m, 2H), 2.46 (s, 3H). ¹³C NMR (100 MHz, CDCl₃) δ 193.7, 134.6, 132.6, 132.2, 132.1, 128.9, 124.6, 124.4, 121.8, 91.6, 90.7, 30.7. HRMS calcd for C₂₄H₁₁F₅OS, 442.0451; found, 442.0459.



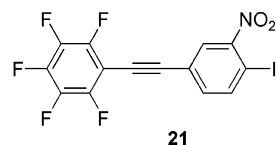
4.13. 4-(4-Pentafluorophenylethynylphenylethynyl)benzenethiol (1). Following the general deprotection of arylthioacetates, **16** (230 mg, 0.5 mmol) was dissolved in CH₂Cl₂ and MeOH (40 mL each), with H₂SO₄ (10 drops). Flash chromatography (1:1, hexanes/CH₂Cl₂) afforded the desired product (98 mg, 50% yield) as a yellow solid; mp 228–232 °C. IR (KBr) 2921, 2853, 2547, 2466, 2431, 2205, 1926, 1600, 1526, 1494, 1446, 1402, 1355, 1258, 1106 cm⁻¹. ¹H NMR (400 MHz, CDCl₃) δ 7.53 (m, 4H), 7.41 (m, 2H), 7.25 (m, 2H), 3.54 (s, 1H), 3.58 (s, 1H). ¹³C NMR (100 MHz, CDCl₃) δ 136.4, 132.6, 132.4, 132, 131.7, 129.9, 129.1, 126.8, 126.5, 124.7, 121.3, 120.1, 101.3, 100.3, 91.7, 89.4. HRMS calcd for C₂₂H₉F₅S, 400.0345; found, 400.0340.



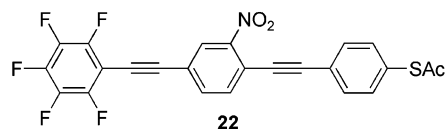
4.14. 4-Ethynyl-2-nitrophenylamine (19). Following the general deprotection of TMS-alkynes, **18**⁵² (1.45 mg, 6.1 mmol) was dissolved in a mixture of CH₂Cl₂ (14 mL), MeOH (12 mL), and K₂CO₃ (3.42 g, 24.0 mmol). Flash chromatography (3:1, hexanes/CH₂Cl₂) afforded the desired product (0.9 g, 88% yield) as a bright yellow solid; mp 193–198 °C. IR (KBr) 3490, 3373, 3255, 2547, 2434, 2330, 1629, 1546, 1511, 1461, 1407, 1358, 1253, 1155, 1078 cm⁻¹. ¹H NMR (400 MHz, CDCl₃) δ 8.28 (d, *J* = 2 Hz, 1H), 7.43 (dd *J* = 8.8, 2 Hz, 1H), 6.77 (d, *J* = 8.8 Hz, 1H), 6.26 (br s, 2H), 3.01 (s, 1H). ¹³C NMR (100 MHz, CDCl₃) δ 144.7, 138.7, 130.4, 119, 110.8, 82.00. HRMS calcd for C₈H₆N₂O₂, 162.0429; found, 162.0429.



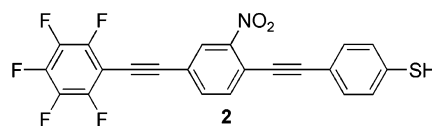
4.15. 2-Nitro-4-pentafluorophenylethynylaniline (20). Following the Sonogashira coupling protocol, **19** (6.2 g, 38.0 mmol), bromopentafluorobenzene (19.1 g, 77.0 mmol), PdCl₂(PPh₃)₂ (1.0 g, 4.3 mol), and CuI (0.6 g, 8.6 mmol) were dissolved in THF (100 mL). Hünig's base (27 mL, 154.0 mmol) was added and the reaction was stirred overnight at 70 °C. Purification by flash chromatography (CH₂Cl₂) afforded the desired product (3.7 g, 30% yield) as a dark yellow solid; mp 216–220 °C.; IR (KBr) 3468, 3364, 3099, 2221, 1631, 1502, 1338, 1243, 1163, 1117 cm⁻¹. ¹H NMR (400 MHz, CDCl₃) δ 8.32 (s, 1H), 7.62 (d, *J* = 8.8 Hz, 1H), 7.53 (br s, 2H), 7.21 (d, *J* = 8.8 Hz, 1H). ¹³C NMR (100 MHz, CDCl₃) δ 205.7, 148.7, 138, 130.1, 120.3, 108.4, 100.8. HRMS calcd for C₁₄H₅F₅N₂O₂, 328.0271; found, 328.0271.



4.16. 2-Iodo-5-pentafluoronitrobenzene (21). Following the general iodination procedure via diazotization, BF₃·Et₂O (7.0 g, 49.0 mmol) was added to a solution of **20** (1.7 g, 12.0 mmol) in THF (20 mL), followed by the addition of isoamyl nitrite (6.0 mL, 43.0 mmol). After the benzenediazonium tetrafluoroborate was isolated, it was added into a solution of NaI (1.4 g, 5.0 mmol) and I₂ (1.2 g, 5.0 mmol) in CH₃CN (8 mL). Flash chromatography (2:1, hexanes/CH₂Cl₂) gave the desired product (2.1 g, 39% yield); mp 126–128 °C. IR (KBr) 3092, 2879, 2229, 1526, 1499, 1518, 1442, 1356, 1356, 1112, 1017 cm⁻¹. ¹H NMR (400 MHz, CDCl₃) δ 8.09 (d, *J* = 8.4 Hz, 1H), 8.03 (d, *J* = 2 Hz, 1H). ¹³C NMR (100 MHz, CDCl₃) δ 165.9, 142.4, 135.8, 128.3, 123.2, 117.7, 89.6, 87.8. HRMS calcd for C₁₄H₃F₅INO₂, 438.9128; found, 438.9120.

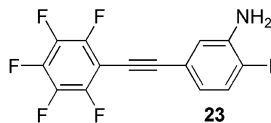


4.17. Thioacetic acid 4-(2-nitro-4-pentafluorophenylethynylphenylethynyl)benzenethiol (22). Following the Sonogashira coupling protocol, **21** (250 mg, 1.4 mmol), **15**²⁵ (287 mg, 1.6 mmol), PdCl₂(PPh₃)₂ (104 mg, 0.6 mmol), and CuI (57 mg, 1.2 mmol) were dissolved in THF (15 mL). TEA (0.7 mL, 6.0 mmol) was added and the reaction was stirred overnight at room temperature. Purification by flash chromatography (1:1, hexanes/CH₂Cl₂) afforded the desired product (350 mg, 49% yield) as a yellow solid; mp 183–188 °C. IR (KBr) 3086, 2916, 2858, 2438, 2208, 1930, 1698, 1606, 1530, 1493, 1442, 1348, 1266, 1121 cm⁻¹. ¹H NMR (400 MHz, CDCl₃) δ 8.29 (d, *J* = 1.2 Hz, 1H), 7.76 (m, 2H), 7.63 (m, 2H), 7.45 (m, 2H), 2.46 (s, 3H). ¹³C NMR (100 MHz, CDCl₃) δ 193.2, 135.6, 134.9, 134.4, 132.8, 130, 128.1, 123.2, 119.4, 99.1, 86.1, 30.5. HRMS calcd for C₂₄H₁₀F₅NO₂S, 487.0301; found, 487.0300.

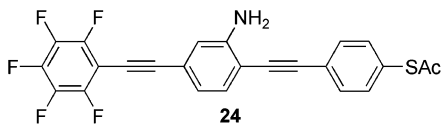


4.18. 4-(2-Nitro-4-pentafluorophenylethynylphenylethynyl)benzenethiol (2). Following the general deprotection of arylthioacetates, **22** (255 mg, 0.5 mmol) was dissolved in CH₂Cl₂ and MeOH (5 mL each), with concentrated H₂SO₄ (5 drops). Flash chromatography (1:1, hexanes/CH₂Cl₂) afforded the desired product

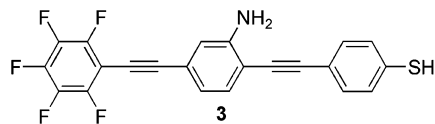
(88 mg, 48% yield) as a yellow solid; mp 228–232 °C (decomp). IR (KBr) 3087, 3033, 2210, 1902, 1591, 1533, 1494, 1444, 1346, 1346, 1267, 1102 cm^{-1} . ^1H NMR (400 MHz, CDCl_3) δ 8.28 (d, J = 1.2 Hz, 1H), 7.76 (m, 2H), 7.46 (m, 2H), 7.28 (m, 3H), 3.59 (s, 1H). ^{13}C NMR (100 MHz, CDCl_3) δ 135.6, 134.7, 134.4, 132.9, 128.9, 128.2, 122.1, 119.7, 119.1, 99.82, 85.3. HRMS calcd for $\text{C}_{22}\text{H}_8\text{F}_5\text{NO}_2\text{S}$, 445.0196; found, 445.0191.



4.19. 2-Iodo-5-pentafluorophenylethynylphenylamine (23). Into a 50-mL round-bottom flask, **21** (300 mg, 0.6 mmol) was dissolved in EtOAc (4 mL) before adding $\text{SnCl}_4 \cdot \text{H}_2\text{O}$ (617 mg, 2.7 mmol). The reaction mixture was heated at reflux for 2 h, and after cooling, the mixture was dissolved in $\text{CH}_2\text{Cl}_2 \cdot \text{H}_2\text{O}$ (400 mL), followed by extractions with CH_2Cl_2 . The organic layers were combined and dried over MgSO_4 , followed by filtration and solvent removal in vacuo. Flash chromatography (2:1, hexanes/ CH_2Cl_2) afforded the desired product (175 mg, 63% yield) as a bright yellow solid; mp 158–162 °C. IR (KBr) 3452, 3367, 2920, 2222, 2178, 1612, 1496, 1449, 1407, 1107 cm^{-1} . ^1H NMR (400 MHz, CDCl_3) δ 7.66 (d, J = 8 Hz, 1H), 6.93 (s, 1H), 6.67 (dd, J = 8, 1.6 Hz, 1H), 4.02 (br s, 2H). ^{13}C NMR (100 MHz, CDCl_3) δ 147, 139.3, 123.1, 122.6, 117.1, 86, 73.5. HRMS calcd for $\text{C}_{14}\text{H}_5\text{F}_5\text{IN}$, 408.9386; found, 408.9388.

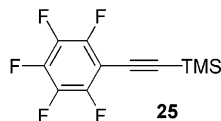


4.20. Thioacetic acid 4-(2-amino-4-pentafluorophenylethynylphenylethynyl)phenyl ester (24). Following the Sonogashira coupling protocol, **23** (868 mg, 1.9 mmol), **15**²⁵ (384 mg, 2.1 mmol), $\text{PdCl}_2(\text{PPh}_3)_2$ (139 g, 0.2 mmol), and CuI (75 mg, 0.4 mmol) were dissolved in THF (15 mL). TEA (1.1 mL, 7.9 mmol) was added and the reaction was left overnight at room temperature. Purification by flash chromatography (1:2, hexanes/ CH_2Cl_2) afforded the desired product (360 mg, 38% yield) as a yellow solid; mp 216–220 °C. IR (KBr) 3476, 3372, 3060, 3025, 2908, 2205, 1895, 1687, 1609, 1512, 1448, 1420, 1258, 1120 cm^{-1} . ^1H NMR (400 MHz, CDCl_3) δ 7.58 (m, 2H), 7.39 (m, 3H), 6.97 (m, 2H), 4.21 (br s, 2H), 2.46 (s, 3H). ^{13}C NMR (100 MHz, CDCl_3) δ 193.5, 147.8, 132.5, 132.2, 128.6, 124.2, 121.7, 117.3, 109.2, 96.2, 87.1, 30.5. HRMS calcd for $\text{C}_{24}\text{H}_{12}\text{F}_5\text{NOS}$, 457.0559; found, 457.0559.

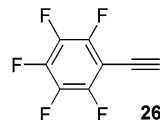


4.21. 4-(2-Amino-4-pentafluorophenylethynylphenylethynyl)benzenethiol (3). Following the general deprotection of arylthioacetates, **24** (165 mg, 0.3 mmol) was dissolved in CH_2Cl_2 and MeOH (20 mL each) with concentrated H_2SO_4 (5 drops). Flash chromatography (1:2, hexanes/ CH_2Cl_2) afforded the desired product (40 mg, 28% yield) as a yellow solid; mp 203–207 °C (decomp). IR (KBr) 3499, 3400, 2923, 2846, 2532, 2213, 1902, 1607, 1525, 1492, 1259, 1107 cm^{-1} . ^1H NMR (400 MHz, CDCl_3) δ 7.40 (m, 2H), 7.25 (m, 2H), 6.96 (m, 3H), 4.42 (br s, 2H), 3.55 (s, 1H). ^{13}C NMR (100 MHz, CDCl_3) δ 150.2, 147.6, 136.4, 132.5, 129.9, 129.1,

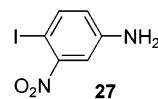
126.8, 126.5, 122.4, 121.7, 120.1, 117.2, 109.6, 96.5, 85.9. HRMS calcd for $\text{C}_{22}\text{H}_{10}\text{F}_5\text{NS}$, 415.0454; found, 415.0461.



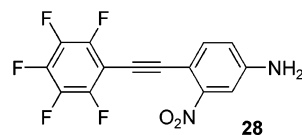
4.22. Trimethylpentafluorophenylethynylsilane (25). Following the Sonogashira coupling protocol, bromopentafluorobenzene (20.0 g, 81.0 mmol), $\text{PdCl}_2(\text{PPh}_3)_2$ (1.1 g, 1.6 mmol), and CuI (0.6 g, 3.2 mol) were dissolved in THF (200 mL). Hünig's base (57 mL, 0.3 mol) was added, followed by TMSA (23.0 mL, 162.0 mmol), and the mixture was stirred for 24 h at 70 °C. Purification by flash chromatography (hexanes) afforded the desired product (15.2 g, 71% yield) as a clear liquid. IR (neat) 3021, 2964, 2902, 2172, 2067, 1620, 1514, 1254, 1216, 1141 cm^{-1} . ^1H NMR (400 MHz, CDCl_3) δ 0.30 (s). ^{13}C NMR (100 MHz, CDCl_3) δ 109.4, 87.4, -0.41. HRMS calcd for $\text{C}_{11}\text{H}_9\text{F}_5\text{Si}$, 264.0393; found, 264.0393.



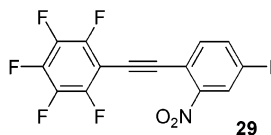
4.23. 1-Ethynyl-2,3,4,5,6-pentafluorobenzene (26). TMS-alkyne **25** (39.7 g, 150.0 mmol) was dissolved in MeOH, and KOH (50%, 0.2 mL) was added. The exothermic reaction was stirred for 10 min before quenching with H_2O (200 mL) and acidifying with HCl (10%, 11 mL) in order to collect a yellow precipitate. Distillation (130 °C, 1 atm) gave a clear, light liquid (25 g, 87%) as the desired product. IR (neat) 3313, 2955, 2778, 2640, 2467, 2436, 2129, 2041, 1639, 1495, 1316, 1262, 1128, 1083 cm^{-1} . ^1H NMR (400 MHz, CDCl_3) δ 3.61 (s). ^{13}C NMR (100 MHz, CDCl_3) δ 89.8, 67.4, 53.5. HRMS calcd for C_8HF_5 , 191.9998; found, 191.9998.



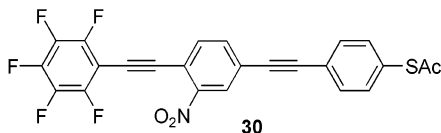
4.24. 4-Iodo-3-nitrophenylamine (27). Into a 500-mL round-bottom flask, 3-nitroaniline (10.0 g, 72.4 mmol) was suspended in a solution of AcOH (200 mL) and NaOAc (40.0 g, 110 mmol). The reaction mixture was cooled to 0 °C and ICl (18.0 g, 110 mmol) was added. The mixture was allowed to warm to room temperature overnight. Saturated $\text{Na}_2\text{S}_2\text{O}_3$ (200 mL) was added and the mixture was stirred until precipitation was observed. After filtration, the orange solid was washed with water and dissolved in acetone, followed by slow addition of hexanes. The precipitate was purified by flash chromatography (CH_2Cl_2 , then 1:1, hexanes/acetone), affording the desired product (7.6 g, 41%) as a dark yellow solid; mp 118–122 °C. IR (KBr) 3426, 3317, 3200, 2085, 2893, 2641, 1622, 1511, 1341, 1097 cm^{-1} . ^1H NMR (400 MHz, $(\text{CD}_3)_2\text{CO}$) δ 7.81 (d, J = 8.2 Hz, 1H), 7.52 (d, J = 2.4 Hz, 1H), 6.98 (dd, J = 8.2, 2.4 Hz, 1H), 5.89 (s, 2H). ^{13}C NMR (100 MHz, $(\text{CD}_3)_2\text{CO}$) δ 149.8, 148.3, 139.4, 111, 106.7, 90.9. HRMS calcd for $\text{C}_6\text{H}_5\text{IN}_2\text{O}_2$, 263.9396; found, 263.9395.



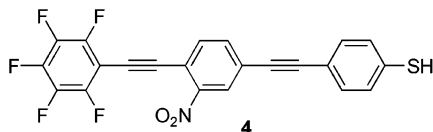
4.25. 3-Nitro-4-pentafluorophenylethynylaniline (28). Following the Sonogashira coupling protocol, **27** (8.5 g, 44.0 mmol), **26**⁵³ (11.6 g, 44.0 mmol), PdCl₂(PPh₃)₂ (620 mg, 0.8 mmol), and CuI (340 mg, 1.6 mmol) were dissolved in THF (150 mL). TEA (25.0 mL, 177.0 mmol) was added and the reaction was stirred overnight. Purification by flash chromatography (CH₂Cl₂) afforded the desired product (3.4 g, 24% yield) as a dark yellow solid; mp 138–142 °C. IR (KBr) 3480, 3358, 2310, 2217, 1632, 1500, 1345, 1249, 1169, 1117 cm⁻¹. ¹H NMR (400 MHz, CDCl₃) δ 7.54 (d, *J* = 8.4 Hz) 7.49 (d, 1H), 7.40 (d, *J* = 2.4 Hz, 1H), 6.88 (dd, *J* = 8.4, 2.4 Hz, 1H), 4.27 (br s, 2H). ¹³C NMR (100 MHz, CDCl₃) δ 148.3, 138.8, 136.3, 126.1, 118.8, 110.1, 97.6, 93.5. HRMS calcd for C₁₄H₅F₅N₂O₂, 328.0271; found, 328.0275.



4.26. 5-Iodo-2-pentafluorophenylethynynitrobenzene (29). Following the general iodination procedure via diazotization, **28** (3.0 g, 9.1 mmol) was dissolved in CH₃CN (25 mL) and added to a solution of NOBF₄ (1.7 g, 10.0 mmol) in CH₃CN (15 mL). After the benzenediazonium tetrafluoroborate was isolated, it was added to a solution of NaI (2.8 g, 18.2 mmol) and I₂ (3.5 g, 13.7 mmol) in CH₃CN (20 mL). Flash chromatography (1:1, hexanes/CH₂Cl₂), gave the desired product (3 g, 75% yield); mp 176–180 °C. IR (KBr) 3083, 2217, 1625, 1519, 1436, 1340, 1276, 1110, 1031 cm⁻¹. ¹H NMR (400 MHz, CDCl₃) δ 8.52 (d, *J* = 1.6 Hz, 1H) 8.00 (dd, *J* = 8.4, 1.6 Hz, 1H), 7.50 (d, *J* = 8.4 Hz, 1H). ¹³C NMR (100 MHz, CDCl₃) δ 149.3, 142.3, 135.9, 134, 116.7, 95.8, 94.7, 81.9. HRMS calcd for C₁₄H₃F₅INO₂, 438.9128; found, 438.9129.

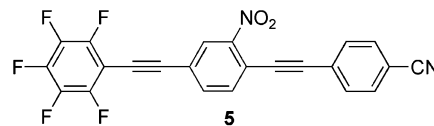


4.27. Thioacetic acid 4-(3-nitro-4-pentafluorophenylethynylphenylethynyl)phenyl ester (30). Following the Sonogashira coupling protocol, **29** (500 mg, 1.1 mmol), **15**²⁵ (201 mg, 1.1 mmol), PdCl₂(PPh₃)₂ (80 g, 0.1 mmol), and CuI (44 mg, 0.2 mmol) were dissolved in THF (25 mL). TEA (0.7 mL, 4.5 mmol) was added and the reaction was stirred at room temperature for 5 h. Purification by flash chromatography (1:1, hexanes/CH₂Cl₂) afforded the desired product (370 mg, 67% yield) as a yellow solid; mp 200 °C. IR (KBr) 3086, 2469, 2411, 2208, 1926, 1708, 1642, 1530, 1492, 1441, 1354, 1227, 1122 cm⁻¹. ¹H NMR (400 MHz, CDCl₃) δ 8.31 (s, 1H), 7.77 (m, 2H), 7.59 (m, 2H), 7.45 (m, 2H), 2.47 (s, 3H). ¹³C NMR (100 MHz, CDCl₃) δ 193.2, 135.7, 135.1, 134.5, 132.5, 129.7, 128, 123.1, 93.8, 88.2, 30.5. HRMS calcd for C₂₄H₁₀F₅NO₃S, 487.0301; found, 487.0305.

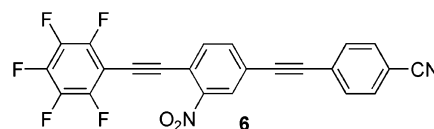


4.28. 4-(3-Nitro-4-pentafluorophenylethynylphenylethynyl)benzenethiol (4). Following the general deprotection of arylthioacetates, **30** (217 mg, 0.4 mmol) was dissolved in CH₂Cl₂ and MeOH (20 mL each), with H₂SO₄ (10 drops). Flash chromatography

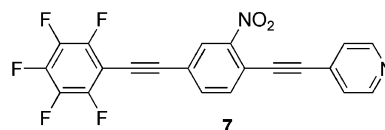
(1:1, hexanes/CH₂Cl₂) afforded the desired product (101 mg, 51% yield) as a yellow solid; mp 228–232 °C (decomp). IR (KBr) 3083, 2916, 2834, 2562, 2209, 1902, 1491, 1443, 1344, 1248, 1098 cm⁻¹. ¹H NMR (400 MHz, CDCl₃) δ 8.27 (m, 1H), 7.74 (m, 2H), 7.42 (m, 2H), 7.27 (m, 2H), 3.58 (s, 1H). ¹³C NMR (100 MHz, CDCl₃) δ 135.6, 135.1, 133.9, 132.5, 129.0, 127.8, 125.9, 119, 116.2, 94.3, 87.2. HRMS calcd for C₂₂H₈F₅NO₂S, 445.0196; found, 445.0194.



4.29. 4-(2-Nitro-4-pentafluorophenylethynylphenylethynyl)benzonitrile (5). Following the Sonogashira coupling protocol, **21** (200 mg, 0.4 mmol), **31**¹⁴ (61 mg, 0.4 mmol), PdCl₂(PPh₃)₂ (32 g, 0.04 mmol), and CuI (18 mg, 0.08 mmol) were dissolved in THF (15 mL). TEA (0.3 mL, 1.8 mmol) was added and the reaction was left at room temperature overnight. Purification by flash chromatography (1:1, hexanes/CH₂Cl₂) afforded the desired product (47 mg, 23% yield) as a yellow solid; mp 238–242 °C (decomp). IR (KBr) 3087, 2224, 1933, 1801, 1604, 1518, 1496, 1442, 1345, 1268, 1115 cm⁻¹. ¹H NMR (400 MHz, CDCl₃) δ 8.32 (d, *J* = 0.8 Hz, 1H), 7.77 (m, 2H), 7.7 (m, 3H), 7.64 (m, 1H). ¹³C NMR (100 MHz, CDCl₃) δ 135.8, 135.0, 133.2, 132.7, 132.4, 132.3, 128.2, 126.3, 118.6, 113.1, 97.4, 88.4. HRMS calcd for C₂₃H₇F₅N₂O₂, 438.0427; found, 438.0439.

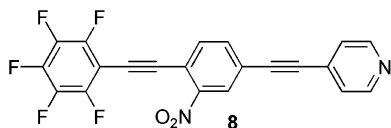


4.30. 4-(3-Nitro-4-pentafluorophenylethynylphenylethynyl)benzonitrile (6). Following the Sonogashira coupling protocol, **29** (200 mg, 0.4 mmol), **31**¹⁴ (61 mg, 0.4 mmol), PdCl₂(PPh₃)₂ (32 mg, 0.04 mmol), and CuI (18 mg, 0.08 mmol) were dissolved in THF (15 mL). TEA (0.3 mL, 1.8 mmol) was added and the reaction was stirred at room temperature overnight. Purification by flash chromatography (1:1, hexanes/CH₂Cl₂) afforded the desired product (90 mg, 46% yield) as a yellow solid; mp 210–214 °C (decomp). IR (KBr) 3090, 2223, 1922, 1606, 1530, 1497, 1443, 1399, 1345, 1269, 1113 cm⁻¹. ¹H NMR (400 MHz, CDCl₃) δ 8.47 (d, *J* = 2.4 Hz, 1H), 8.24 (dd, *J* = 8.4, 2.4 Hz 1H), 7.81 (d, *J* = 8.4, 1H), 7.70 (m, 4H). ¹³C NMR (100 MHz, CDCl₃) δ 147.8, 133.6, 133.2, 132.6, 132.4, 132.3, 130.2, 127.4, 126.6, 126.3, 123.5, 118.4, 113.1, 99.7, 94.5, 89.2, 81.6. HRMS calcd for C₂₃H₇F₅N₂O₂, 438.0427; found, 438.0417.

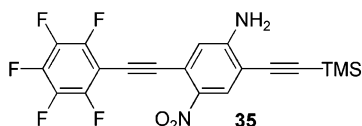


4.31. 4-(2-Nitro-4-pentafluorophenylethynylpyridinylethynyl)pyridine (7). Following the Sonogashira coupling protocol, **21** (230 mg, 0.52 mmol), **32**²⁸ (70 mg, 0.68 mmol), PdCl₂(PPh₃)₂ (25 mg, 0.03 mmol), and CuI (18 mg, 0.09 mmol) were dissolved in THF (30 mL). TEA (15 mL) was added and the mixture was stirred at 65 °C for 16 h. Purification by flash chromatography (4:1, CH₂Cl₂/Et₂O) afforded the desired product (120 mg, 55% yield) as a yellow fluffy solid; mp 175–179 °C. IR (KBr) 3431, 3089, 2227, 1589, 1547, 1521, 1498, 1444, 1408, 1346, 1260, 1215, 1120 cm⁻¹. ¹H NMR (400 MHz, CDCl₃) δ 8.68 (br s, 2H), 8.31 (d, *J* = 1.5 Hz, 1H), 7.81 (dd, *J* = 8.1, 1.5 Hz, 1H), 7.76 (d, *J* = 8.1 Hz, 1H),

7.45 (d, $J = 5.7$ Hz, 2H). ^{13}C NMR (100 MHz, CDCl_3) δ 150.2, 149.9, 135.8, 135.2, 130.3, 128.2, 125.8, 123.4, 118.5, 97.1, 96.3, 88.4. HRMS calcd for $\text{C}_{21}\text{H}_7\text{F}_5\text{N}_2\text{O}_2$, 414.0427; found, 414.0467. Anal. Calcd: C, 60.88; H, 1.70; N, 6.76. Found: C, 60.81; H, 1.59; N, 6.72.

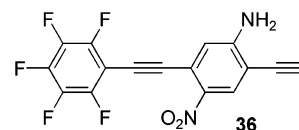


4.32. 4-(3-Nitro-4-pentafluorophenylethynylphenylethynyl)pyridine (8). Following the Sonogashira coupling protocol, **29** (322 mg, 0.73 mmol), **32**²⁸ (91 mg, 0.88 mmol), $\text{PdCl}_2(\text{PPh}_3)_2$ (26 mg, 0.08 mmol), and CuI (14 mg, 0.16 mmol) were dissolved in THF (20 mL). TEA (15 mL) was added and the mixture was stirred at 60 °C for 2 d. Purification by flash chromatography (4:1, $\text{CH}_2\text{Cl}_2/\text{Et}_2\text{O}$) afforded the desired product (78 mg, 26% yield) as a yellow fluffy solid; mp 175–179 °C. IR (KBr) 3094, 2223, 1645, 1590, 1542, 1522, 1498, 1446, 1407, 1348, 1248 cm^{-1} . ^1H NMR (400 MHz, CDCl_3) δ 8.68 (br s, 2H), 8.34 (t, $J = 1.1$ Hz, 1H), 7.80 (m, 2H), 7.42 (m, 2H). ^{13}C NMR (100 MHz, CDCl_3) δ 150.3, 149.5, 135.9, 135.3, 130.2, 128.3, 125.7, 124.7, 117.4, 91.4, 90.6, 82.6. HRMS calcd for $\text{C}_{21}\text{H}_7\text{N}_2\text{O}_2$, 414.0427; found, 414.0427.

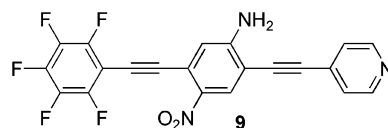


4.33. 4-Nitro-5-pentafluorophenylethynyl-2-trimethylsilyl-ethynylphenylamine (35). Following the Sonogashira coupling protocol, **33** (3.8 g, 13.0 mmol), **26** (2.5 g, 13.0 mmol), $\text{PdCl}_2(\text{PPh}_3)_2$ (370 mg, 0.1 mmol), and CuI (200 mg, 0.2 mmol) were dissolved in THF (150 mL). TEA (7.2 mL, 57.0 mmol) was added and the mixture was stirred at 60 °C for 2 d. Purification by flash chromatography (CH_2Cl_2) afforded an inseparable mixture of mono-adduct and bis-adduct according to HRMS. The bright yellow solid was taken immediately to the next step with no further clean characterization of the mono-adduct. Under the same Sonogashira coupling protocol, the same amounts of $\text{PdCl}_2(\text{PPh}_3)_2$, CuI, and TEA were added and dissolved in THF (100 mL). Excess TMSA (5.0 mL, 35.0 mmol) was added and the reaction mixture was stirred at 60 °C for 2 d. Purification by flash chromatography (2:1, hexanes/ CH_2Cl_2) afforded the desired product **35** (1.4 g, 26% yield over two steps) as a yellow fluffy solid; mp 143–147 °C (decomp). IR (KBr) 3094, 2223, 1645, 1590, 1542, 1522, 1498, 1446, 1407, 1348, 1248 cm^{-1} . ^1H NMR (400 MHz, CDCl_3) δ 8.19 (s, 1H), 7.18 (s, 1H), 5.51 (br s, 2H), 0.32 (s, 9H). ^{13}C NMR (100 MHz, CDCl_3) δ 153.9, 137.8, 131.0, 130.6, 119.0, 118.7, 107.4, 103.7, 99.0, 98.2, 79.4, -0.5. HRMS calcd for $\text{C}_{19}\text{H}_{13}\text{F}_5\text{N}_2\text{O}_2\text{Si}$, 424.066; found, 424.0658.

4.34. 2-Ethynyl-4-nitro-5-pentafluorophenylethynylphenylamine (36). Following the general deprotection of TMS-alkynes, **35** (980 mg, 0.23 mmol) was dissolved in MeOH (20 mL), and



K_2CO_3 (100 mg 0.7 mmol) was added. Purification by flash chromatography (CH_2Cl_2) gave the desired product (750 mg, 93%) as a light yellow solid; mp 243–247 °C (decomp). IR (KBr) 3313, 2955, 2778, 2640, 2467, 2436, 2129, 2041, 1639, 1495, 1316, 1262, 1128, 1083 cm^{-1} . ^1H NMR (400 MHz, CDCl_3) δ 8.21 (s, 1H), 7.17 (s, 1H), 6.45 (br s, 2H), 4.25 (s, 1H). ^{13}C NMR (100 MHz, CDCl_3) δ 154.3, 130.8, 118.7, 106.5, 87.2, 77.9. HRMS calcd for $\text{C}_{16}\text{H}_5\text{F}_5\text{N}_2\text{O}_2$, 352.0271; found, 352.0253.



4.35. 4-Nitro-5-pentafluorophenylethynyl-2-pyridin-4-ylethynylphenylamine (9). Following the Sonogashira coupling protocol, **36** (365 mg, 1.0 mmol), **37**¹⁵ (255 mg, 1.2 mmol), $\text{PdCl}_2(\text{PPh}_3)_2$ (36 mg, 0.01 mmol), and CuI (20 mg, 0.02 mmol) were dissolved in THF (40 mL). TEA (20 mL) was added and the mixture was stirred at 60 °C for 24 h. Purification by flash chromatography (EtOAc) afforded the desired product (206 mg, 46% yield) as a yellow powder; mp slow decomp. IR (KBr) 3442, 3300, 3134, 2212, 1641, 1596, 1546, 1520, 1496, 1318 cm^{-1} . ^1H NMR (400 MHz, $\text{THF}-d_8$) δ 8.60 (br s, 2H), 8.31 (s, 1H), 7.48 (d, $J = 5.2$ Hz, 2H), 6.99 (s, 1H), 6.41 (br s, 2H). ^{13}C NMR (500 MHz, $\text{THF}-d_8$) δ 154.6, 151.1, 138.5, 138.2, 131.7, 131.6, 131.1, 128.0, 126.2, 120.2, 119.6, 107.0, 99.2, 95.1, 88.5. HRMS calcd for $\text{C}_{21}\text{H}_8\text{F}_5\text{N}_3\text{O}_2$, 429.0537; found, 429.0531.

Acknowledgment. This work was funded by the Defense Advanced Research Projects Agency, the Office of Naval Research, and the National Institute of Standards and Testing (U.S. Department of Commerce). The National Science Foundation, CHEM 0075728, provided partial funding for the 400 MHz NMR. We are grateful to R. Stanley Williams and Zhiyong Li of Hewlett-Packard Laboratories QSR, Palo Alto, CA for providing materials and equipment necessary to obtain the FTIR spectrum in Figure 10. We thank Dr. I Chester of FAR Research Inc. for providing trimethylsilylacetylene, and Prof. Jorge Seminario for helpful advice with the DFT calculations.

Supporting Information Available: Material and general procedures, general procedure for coupling of terminal alkynes with aryl halides (Castro-Stephens/Sonogashira protocol), general procedure for alkaline deprotection of TMS-protected alkynes, general procedure for iodination of anilines via diazotization, and general procedure for acid-deprotection of arylthioacetates (pdf). This material is available free of charge via the Internet at <http://pubs.acs.org>.

CM0486161